Defence Research and Development Canada
Recherche et développement pour la défense Canada

ASLAM ROC Analysis Report

Mohsen Ghazel; Stephen Se
MDA
13800 Commerce Parkway
Richmond, B.C.
Canada
V6V 2J3

Contractor's Document Number: ASLAM-RP-53-4754
PWGSC Contract Number: W7702-115043/A
CSA: Jack Collier, 403-544-4871

Defence R&D Canada

Contract Report
DRDC Suffield CR 2013-070

March 2013

Canada

ASLAM ROC Analysis Report

Prepared By:
Mohsen Ghazel; Stephen Se
MDA
13800 Commerce Parkway
Richmond, B.C.
Canada
V6V 2J3

Contractor's Document Number: ASLAM-RP-53-4754
PWGSC Contract Number: W7702-115043/A
CSA: Jack Collier, 403-544-4871

Defence Research and Development Canada – Suffield

Contract Report
DRDC Suffield CR 2013-070
March 2013

IMPORTANT INFORMATIVE STATEMENTS

The scientific or technical validity of this Contract Report is entirely the responsibility of the Contractor and the contents do not necessarily have the approval or endorsement of the Department of National Defence of Canada.

Abstract

The objective of the Appearance-based Simultaneous Localization And Mapping (ASLAM) project is the research and development of an Appearance-Based Simultaneous Localization and Mapping system for day/night operations in indoor and outdoor environments. These algorithms would perform place recognition based on sensor data gathered from an Unmanned Ground Vehicle (UGV) as it travels through the environment. When the vehicle returns to a previously visited scene, the ASLAM algorithm would recognize the scene, update its internal representation, report this to the UGV, and finally provide information to aid in closing the loop with geometric Simultaneous Localization And Mapping (SLAM).

The key objectives of Task 4.4 are to characterize the performance of the ASLAM system under different settings and to determine the optimal system parameters, with detailed Receiver Operator Characteristic (ROC) analysis.

This report describes the findings of the ROC analysis. The ROC curves illustrate graphically how the probability of detection and the false alarm rate vary at different thresholds, and how the key system parameters affect the performance.

Résumé

L'objectif du présent contrat est la recherche et le développement d'un système de localisation et de cartographie en temps réel basé sur l'apparence pour les opérations menées de jour et de nuit, à l'intérieur comme à l'extérieur. Ces algorithmes doivent effectuer une reconnaissance de l'endroit basée sur les données recueillies par le capteur de l'UGV alors que celui-ci se déplace dans un environnement donné. Lorsque le véhicule revient sur une scène déjà visitée, l'algorithme ASLAM reconnaît la scène, met à jour sa représentation interne, la communique au UGV et, enfin, dispose d'un mécanisme pour fermer la boucle à l'aide du SLAM géométrique.

Les principaux objectifs de la tâche 4.4 sont de caractériser le rendement du système ASLAM sous divers réglages et de déterminer les paramètres optimaux du système à l'aide d'une analyse détaillée de la fonction d'efficacité du récepteur (FER).

Le présent rapport comprend les résultats de l'analyse FER. Les courbes de la FER illustrent comment la probabilité de détection et le taux de fausses alarmes varient en fonction de certains seuils et quelle incidence les principaux paramètres du système ont sur le rendement.

This page intentionally left blank.

ASLAM

ROC Analysis Report (Task 4.4)

March 28, 2013

Mohsen Ghazel & Stephen Se

MDA Systems Ltd.

PWGSC Contract Title:	Appearance Based SLAM for Indoor/Outdoor Urban Terrain
MDA Project Title:	6024 - ASLAM
MDA Document Number:	ASLAM-RP-53-4754
Contract No.:	W7702-115043/A
Project Duration:	October 20 2010 – March 31 2013
DRDC Technical Authority:	Mr. Jack Collier (403) 544-4871

13800 Commerce Parkway
Richmond, B.C., Canada, V6V 2J3
Telephone (604) 278-3411
Fax (604) 231-2753

THIS PAGE INTENTIONALLY LEFT BLANK

ASLAM

ROC Analysis Report (Task 4.4)

March 28, 2013

Mohsen Ghazel & Stephen Se

MDA Systems Ltd.
13800 Commerce Parkway
Richmond, BC, Canada
V6V 2J3

PWGSC Contract Title:	Appearance Based SLAM for Indoor/Outdoor Urban Terrain
MDA Project Title:	6024 – ASLAM
MDA Document Number:	ASLAM-RP-53-4754
Contract No.:	W7702-115043/A
Project Duration:	October 20 2010 – March 31 2013
DRDC Technical Authority:	Mr. Jack Collier (403) 544-4871

Prepared By:	Mohsen Ghazel	Mar 27, 2013 Signature and Date
Prepared By:	Stephen Se	Mar 27, 2013 Signature and Date
Project Manager:	Stephen Se	Mar 27, 2013 Signature and Date

MacDonald, Dettwiler and Associates Ltd
13800 Commerce Parkway
Richmond, BC, Canada
V6V 2J3

CHANGE RECORD

ISSUE	DATE	PAGE(S)	DESCRIPTION
1/0	Mar. 28, 2013	All	First Issue

THIS PAGE INTENTIONALLY LEFT BLANK

TABLE OF CONTENTS

1 INTRODUCTION 1-1
1.1 Project Objectives 1-1
1.2 Task 4.4 Objectives 1-1
1.3 Scope 1-1

2 ROC ANALYSIS 2-1
2.1 Selected System Parameters 2-1
2.2 ROC Analysis for Probability Thresholds 2-3
2.2.1 Parameters Setting 2-3
2.2.2 Results and Discussion 2-4
2.3 ROC Analysis for SIFT Parameters 2-8
2.3.1 Parameters Setting 2-8
2.3.2 Results and Discussion 2-9
2.4 ROC Analysis for VD-LSD Parameters 2-12
2.4.1 3-Dimensional Property Vectors 2-15
2.4.2 4-Dimensional Property Vectors 2-18
2.4.3 5-Dimensional Property Vectors 2-21
2.4.4 6-Dimensional Property Vectors 2-24
2.4.5 7-Dimensional Property Vectors 2-30
2.4.6 Minimum E3/E1 Ratio Threshold 2-33
2.4.7 Discussions of the VD-LSD Experimental Results 2-35

3 CONCLUSIONS 3-1
3.1 Summary 3-1
3.2 Recommendations 3-2
3.3 Future Work 3-3

4 REFERENCES 4-1

THIS PAGE INTENTIONALLY LEFT BLANK

LIST OF FIGURES

Figure 2-1 Sensitivity of the Detection Results to the Variability of the Probability Threshold for the 12PM Data Set 2-6
Figure 2-2 Sensitivity of the Detection Results to the Variability of the Probability Threshold for the 4PM Data Set 2-7
Figure 2-3 Sensitivity of the Detection Results to the Variability of the SIFT Scale Threshold for the 12PM Data Set 2-10
Figure 2-4 Sensitivity of the Detection Results to the Variability of the SIFT Scale Threshold for the 4PM Data Set 2-11
Figure 2-5 Sensitivity of the Detection Results to the Selection of the 3-Dimensional VD-LSD properties and Number of Quantization Bins per Dimension for the 12PM Data Set 2-17
Figure 2-6 Sensitivity of the Detection Results to the Variability of the 4-Dimensional VD-LSD Properties and Number of Quantization Bins per Dimension for the 12PM Data Set 2-20
Figure 2-7 Sensitivity of the Detection Results to the Variability of the 5-Dimensional VD-LSD Properties and Number of Quantization Bins per Dimension for the 12PM Data Set 2-23
Figure 2-8 Sensitivity of the Detection Results to the Variability of the 6-Dimensional VD-LSD Properties and Number of Quantization Bins per Dimension for the 12PM Data Set (Approach 1) 2-26
Figure 2-9 Sensitivity of the Detection Results to the Variability of the 6-Dimensional VD-LSD Properties and Number of Quantization Bins per Dimension for the 12PM Data Set (Approach 2) 2-29
Figure 2-10 Sensitivity of the Detection Results to the Variability of the 7-Dimensional VD-LSD Properties and Number of Quantization Bins per Dimension for the 12PM Data Set using 2 Quantization Bins 2-32
Figure 2-11 Sensitivity of the Detection Results to the Variability of the Minimum E3/E1 Ratio Threshold over the [0.01, 0.2] Range, for the 12PM Data Set 2-34
Figure 2-12 The Selected Properties for the Best Experimental Results for the Different VD-LSD vector Dimensions and Number of Quantization Bins 2-36
Figure 2-13 The Probability of Detection for the Best Experimental Results for the Different VD-LSD Vector Dimensions and Number of Quantization Bins 2-37
Figure 2-14 Execution Times (including Vocabulary Generation) for the 6-Dimensional VD-LSD Vector using 2 and 3 Histogram Quantization Bins (on the ASLAM Linux Server Machine) 2-38

THIS PAGE INTENTIONALLY LEFT BLANK

LIST OF TABLES

Table 2-1 Tested System Parameters 2-3
Table 2-2 Tested System Parameters Setting for Variable Probability Threshold 2-4
Table 2-3 Tested System Parameters Setting for Variable SIFT Scale Threshold 2-8
Table 2-4 Tested System Parameters Setting for Variable VD-LSD Parameters 2-12
Table 2-5 The VD-LSD Properties 2-13
Table 2-6 3-Dimensional VD-LSD Properties Selection 2-15
Table 2-7 Randomly Selected 3-Dimensional Property Vectors 2-15
Table 2-8 Best Experimental Results for 3-Dimensional VD-LSD 2-18
Table 2-9 4-Dimensional VD-LSD Properties Selection 2-18
Table 2-10 Randomly Selected 4-Dimensional Property Vectors 2-18
Table 2-11 Best Experimental Results for 4-Dimensional VD-LSD 2-21
Table 2-12 5-Dimensional VD-LSD Properties Selection 2-21
Table 2-13 Randomly Selected 5-Dimensional Property Vectors 2-22
Table 2-14 Best Experimental Results for 5-Dimensional VD-LSD 2-24
Table 2-15 6-Dimensional VD-LSD Properties Selection (Approach 1) 2-24
Table 2-16 Randomly Selected 6-Dimensional Property Vectors (Approach 1) 2-25
Table 2-17 Best Experimental Results for 6-Dimensional VD-LSD (Approach 1) 2-27
Table 2-18 6-Dimensional VD-LSD Properties Selection (Approach 2) 2-27
Table 2-19 Randomly Selected 6-Dimensional Property Vectors (Approach 2) 2-28
Table 2-20 Best Experimental Results for 6-Dimensional VD-LSD (Approach 2). 2-30
Table 2-21 7-Dimensional VD-LSD Properties Selection 2-30
Table 2-22 Randomly Selected 7-Dimensional Property Vectors 2-31
Table 2-24 Tested System Parameters Settings for Variable Minimum E3/E1 Ratio Threshold 2-33
Table 2-25 Best Experimental Results for the Different VD-LSD Vector Dimensions and Number of Quantization Bins 2-35
Table 2-26 Default VD-LSD Parameters Setting 2-36
Table 2-27 Common VD-LSD Properties Yielding the Best Experimental Results 2-37
Table 3-1 Recommended Tested ASLAM System Parameters Settings 3-2

THIS PAGE INTENTIONALLY LEFT BLANK

ACRONYMS AND ABBREVIATIONS

API	Application Programming Interface
ASLAM	Appearance-based Simultaneous Localization And Mapping
DOF	Degrees Of Freedom
DRDC	Defence Research & Development Canada
FAB-MAP	Fast Appearance Based Mapping
LIDAR	Light Detection and Ranging
MDA	MDA Systems Ltd.
PD	Probability of Detection
PFA	Probability of False Alarm
ROC	Receiver Operating Characteristics
SIFT	Scale Invariant Feature Transform
SLAM	Simultaneous Localization And Mapping
UGV	Unmanned Ground Vehicle
VD-LSD	Variable Dimensional Local Shape Descriptor

THIS PAGE INTENTIONALLY LEFT BLANK

1 INTRODUCTION

1.1 Project Objectives

The objective of the Appearance-based Simultaneous Localization And Mapping (ASLAM) project is the research and development of an Appearance-Based Simultaneous Localization and Mapping system for day/night operations in indoor and outdoor environments. These algorithms would perform place recognition based on sensor data gathered from an Unmanned Ground Vehicle (UGV) as it travels through the environment. When the vehicle returns to a previously visited scene, the ASLAM algorithm would recognize the scene, update its internal representation, report this to the UGV, and finally provide information to aid in closing the loop with geometric Simultaneous Localization And Mapping (SLAM).

1.2 Task 4.4 Objectives

This project has developed and delivered a multi-sensor ASLAM system that is capable of scene recognition, as described in the final report [R-2]. While the system works well during the field trials, it is not clear whether it is producing optimal results and if not, what the optimal system parameters are, as there are a number of configurable parameters in the system.

The key objectives of Task 4.4 are to characterize the performance of the ASLAM system under different settings and to determine the optimal system parameters, with detailed Receiver Operator Characteristic (ROC) analysis.

1.3 Scope

This report document is to fulfil Task 4.4 milestone of the contract [R-1] and describes the findings of the ROC analysis. The ROC curves illustrate graphically how the probability of detection and the false alarm rate vary at different thresholds, and how the key system parameters affect the performance.

THIS PAGE INTENTIONALLY LEFT BLANK

2 ROC ANALYSIS

The ASLAM system parameters have been set to their default values based on a limited level of experimentation. Typically, there is a trade-off between the rate of true scene detection and the rate of false alarm, while adjusting some of the key system parameters. For example, reducing the detection threshold should increase the probability of detection but may also increase the false alarm rate. Therefore, a more detailed experimentation and sensitivity analysis of the key system parameters are needed in order to select more optimized values for these parameters and attain sufficient detection rate, while keeping the false alarm rate low. The sensitivity analysis is presented in this section using Receiver Operating Characteristic (ROC) curves.

A ROC curve is a graphical plot which illustrates the performance of a binary classifier system as one of its discrimination thresholds is varied. It is created by plotting the probability of true detection as a function of the probability of false alarm, at various threshold settings.

In this section, we illustrate various ROC curves generated by varying a selected set of ASLAM system parameters, as discussed next.

2.1 Selected System Parameters

In this section, we examine the sensitivity of the loop detection results to the variability of selected set of system parameters of the following key components of the ASLAM system:

1. Fast Appearance Based Mapping (FAB-MAP) recognition engine: One of the key parameters of this engine is the probability of detection threshold, where scene detection is flagged if its probability of being an actual detection is greater or equal to this threshold. Currently, a value of 0.99 is used as the FAB-MAP probability threshold to be considered as scene recognition. A ROC curve generated by varying this parameter will illustrate how the probability of detection and false alarm rate vary at different threshold values. This may allow us to fine-tune this threshold parameter and identify a more optimized value of the probability threshold than the currently used default value, if possible.

2. Scale Invariant Feature Transform (SIFT): An image-based SIFT feature is identified by its location and scale, in the set of scale space images. Currently, SIFT features of scale less than a SIFT scale threshold of 2.0 are not used. Such small-scale features often correspond to small attributes on the ground, such as gravel. Hence, these small-scale features are generally not sufficiently distinctive features and may not be suitable for recognition. An experimental analysis of the sensitivity of the loop detection results to the variation of this SIFT scale threshold will help fine-tune this parameter.

3. Variable Dimensional Local Shape Descriptor (VD-LSD): There are 25 possible VD-LSD properties, which can be computed from a point cloud [R-3]. Currently, the default VD-LSD properties vector consists of 6 of the 25 properties with two quantization bins for each dimension, resulting in a feature vector of 64 elements. There are a number of system parameters settings related to the VD-LSD. Our experimental analysis will focus on the following parameters:

    - The dimension and value of the property vector: By default, the selected 6-dimensional property vector is based on previous RADARSAT pose estimation work done at MDA Brampton[R-3] [R-4]. However, there is a need to conduct a more detailed experimental examination of the dependence of the loop detection results on the selected VD-LSD property vector. Therefore, performance analysis may help determine more optimal dimensions for the type of urban and rural scenes encountered in this project.

    - The number of quantization (histogram) bins for each dimension: By default, we only use two histogram bins, which reduces the distinctiveness of the feature vector, but using more bins would spread out the feature vector distribution with additional computation cost. Therefore, a more detailed experimental analysis, which involves the use of different number of quantization bins, may help determine more optimal bin size for each dimension.

    - There are also a number of eigenvalue thresholds used during the VD-LSD extraction, such as E3/E1 ratio, E3/E2 ratio and E2/E1 ratio, which determine whether a 3D point should be considered a salient feature. Each point has three eigenvalues (E1, E2, E3) if there are more than 2 points found in its neighborhood. The three eigenvalues are sorted in a decreasing order of magnitude, as E1 > E2 > E3. In this experimental study, we examine the significance of the E3 to E1 ratio threshold, min*_abs_E3_to_E1,* parameter, which is a threshold to filter out feature points. If (E3 / E1) is less than *min_abs_E3_to_E1*, this point will be excluded from histogram calculation, because it is on a flat surface. If set this value to zero, this condition will be disabled. Currently, the *min_abs_E3_to_E1* threshold parameter is set to 0.1. A more detailed experimental analysis may help fine-tune this parameter.

Table 2-1 summarizes the ASLAM system parameters, which are selected for experimental analysis. For each selected system parameter, we generate ROC curves by varying the parameter over a feasible range, while keeping all other parameters fixed. This will allow us to assess the sensitivity of the detection results to the varied parameter only, as all other parameters settings are fixed. As discussed later, the generated ROC curves will allow us to determine if the default settings of these system parameters are reasonably optimal and identify more optimal values for these parameters, whenever possible.

Table 2-1 Tested System Parameters

System Component	Parameter	Default Value
FAB-MAP	Probability threshold	0.99
SIFT	SIFT scale threshold	2.0
VD-LSD	LSD property vector dimension	6
	LSD property vector (selected properties)	[10, 13, 14, 20, 21, 22]
	Number of quantization bins per dimension	2
	Minimum E3/E1 ratio	0.1

Next, we begin by generating ROC curves by varying the probability threshold parameter of the FAB-MAP engine.

2.2 ROC Analysis for Probability Thresholds

As mentioned in the previous section, the default value of the FAB-MAP probability threshold has been set to 0.99, In this section, we vary this parameter, while keeping all other system settings fixed, in order to examine the sensitivity of the scene detection results to the variation of this parameter only, and perhaps identify a more optimal default value for this parameter.

2.2.1 Parameters Setting

Table 2-2 illustrates the setting of the systems parameters for examining the sensitivity of the detection results to the variability of the FAB-MAP recognition engine probability threshold parameter and generating the corresponding ROC curves.

Note the following:

- All other systems parameters of interest are fixed at their default values. This will allow us to assess the effects of varying on the probability threshold on the detection results.
- Since this detection probability threshold is used as the critical value for all detection from video imagery as well as Light Detection and Ranging (LIDAR) data, varying this parameter will affect the detection results generated from optical imagery as well as the results generated from LIDAR data.
- Since the training vocabulary does not depend on this parameter, the same training vocabulary generated for the default values of the SIFT scale threshold and the VD-LSD property vector, is used for all iterated values of the probability threshold parameter.
- Two data sets from Aug 20, 2012 are used for this analysis:
  - 12 PM Data Set: This is considered as an “optimal” data set because of the “ideal” weather, sun-light angle (mid-day) and illumination conditions during the acquisition of the optical data.

- 4 PM Data Set: This data set is of a lesser quality than the 12 PM data set, as it was acquired later in the day and under less favourable sun-light conditions.

Table 2-2 Tested System Parameters Setting for Variable Probability Threshold

System Component	Parameter	Variability	Initial Value	Step Size	Final Value	Default Value
FAB-MAP	Probability threshold	Iterated	0.70 (12PM) 0.80 (4PM)	0.01	0.99	
SIFT	SIFT scale threshold	Fixed				2.0
VD-LSD	LSD property vector dimension	Fixed				6
	LSD property vector selected properties	Fixed				[10, 13, 14, 20, 21, 22]
	Number of quantization bins per dimension	Fixed				2
	Minimum E3/E1 ratio	Fixed				0.1

The experimental results are illustrated and discussed next.

2.2.2 Results and Discussion

Figure 2-1 and Figure 2-2 illustrate the experimental results, generated by varying the probability threshold parameter while keeping all other selected system parameters, as indicated in Table 2-2, for the 12 PM and 4PM data sets, respectively. For each figure:

- The top graph shows a ROC scatter plot of the probability of detection vs. the probability of false alarm, for each tested probability threshold value.
- The bottom graph illustrates the dependence of the probability of detection on the selected value of the probability threshold.

In view of these results, we make the following observations:

- We almost always have a zero probability of false alarm, with the exception of the LIDAR only results when using the 4PM data where a very low probability of false alarm is observed for some values of the probability threshold. This is likely due to the fact that most, if not all, of the false FAB-MAP loop detections, which are false alarms, are often rejected by 6 Degrees Of Freedom (DOF) validation of the ASLAM Application Programming Interface (API). When visualizing the detection results, we often observe the green dot being plotted, indicating FAB-MAP loop detections, which were rejected by the ASLAM API 6 DOF validation post-processing operation. We should also add here that, throughout this experimental study, a detection is deemed to be a true detection if the computed distance offset is less than or equal to 20 m.

- For both data sets and for all values of the probability threshold, the order of performance, from best to worst, of the various combination is as follows:
  1. Image OR LIDAR
  2. Image only
  3. LIDAR only
  4. Image AND LIDAR
- The image-based results are slightly better for the 12PM data set as compared to the 4PM data set. This is to be expected, as the 12PM data set was acquired under better illumination and visibility conditions.
- The LIDAR results for the two data sets are comparable, as expected since LIDAR results should not depend on weather or illumination conditions.
- For 12PM data set, the probability of detection starts to decrease for larger values of the probability threshold, exceeding 0.95. This observation also hold for the 4PM data set, except for the LIDAR only based results, which appear to be unaffected by larger value of the probability threshold parameter.
- Based on these experimental results, the default value of the probability threshold parameter should be set to about 0.95 instead of 0.99, as this value yields slightly better image-based detection results.

This completes the experimental analysis of the probability threshold parameter. Next, we examine the effects of varying the SIFT scale threshold parameter.

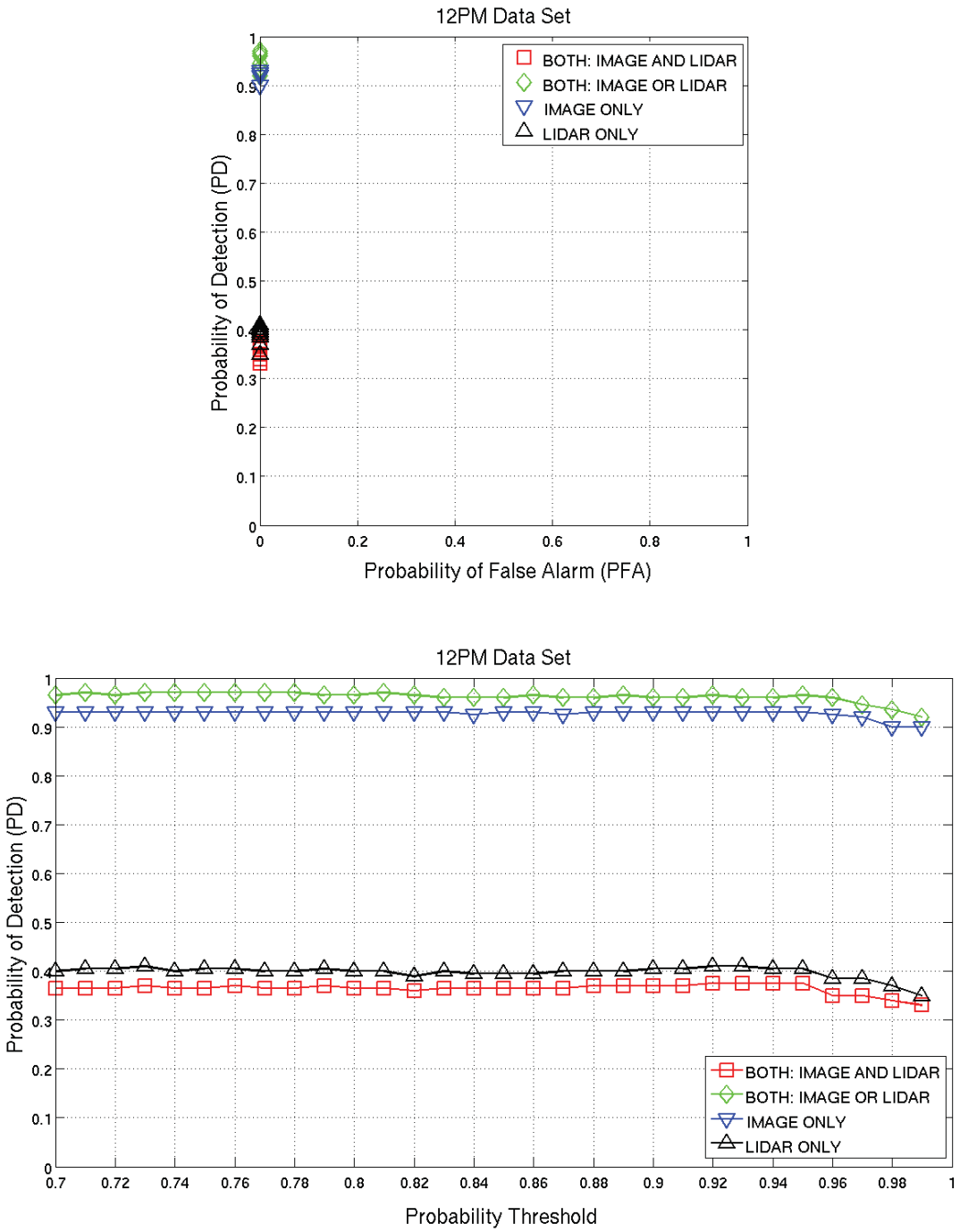

Figure 2-1 Sensitivity of the Detection Results to the Variability of the Probability Threshold for the 12PM Data Set

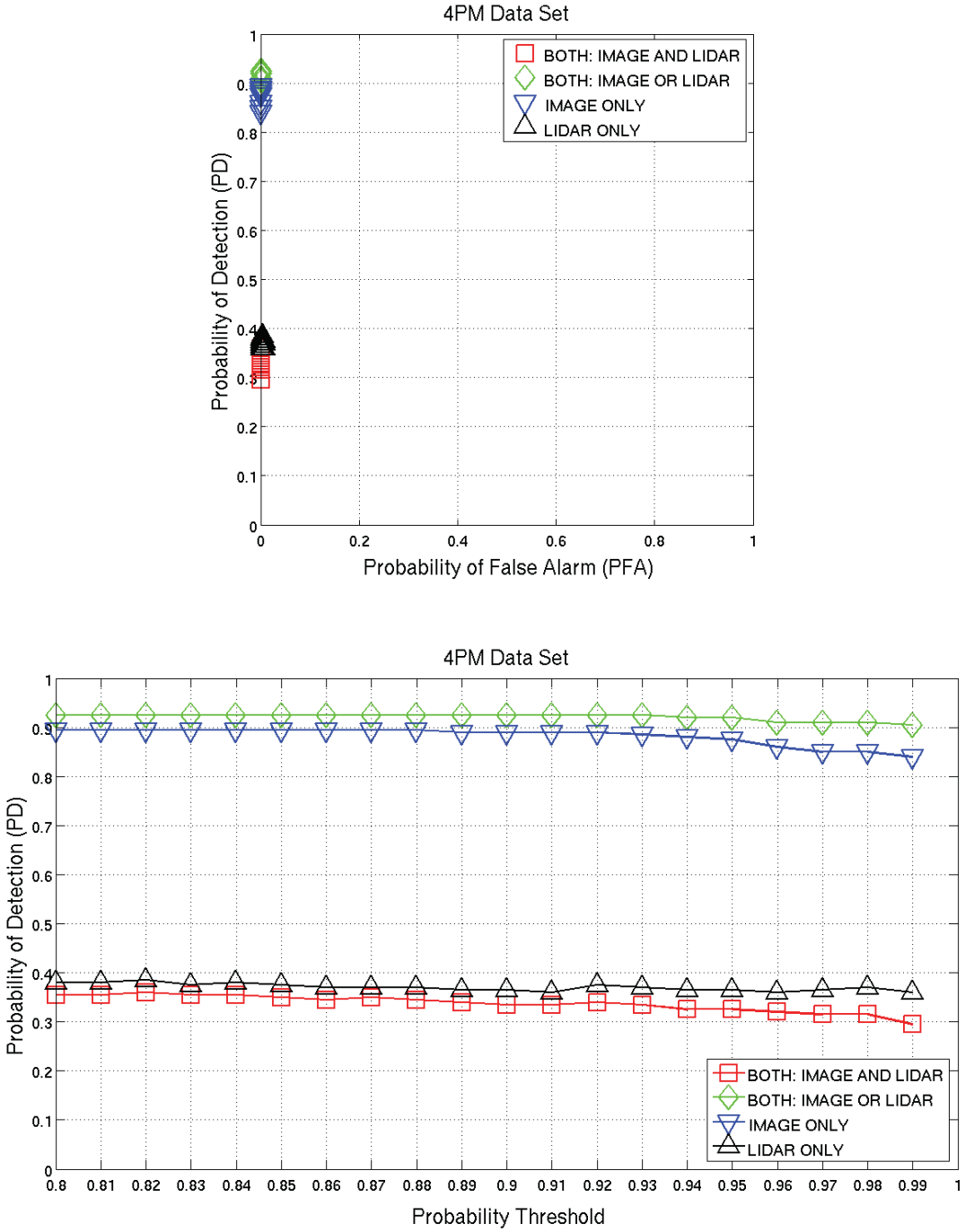

Figure 2-2 Sensitivity of the Detection Results to the Variability of the Probability Threshold for the 4PM Data Set

2.3 ROC Analysis for SIFT Parameters

As mentioned in the previous section, the default value of the SIFT scale threshold has been set to 2.0, In this section, we vary this parameter, while keeping all other system settings fixed, in order to examine the sensitivity of the scene detection results to the variation of this parameter and perhaps identify a more optimal default value for this parameter.

2.3.1 Parameters Setting

Table 2-3 illustrates the setting of the systems parameters for examining the sensitivity of the detection results to the variability of the SIFT scale threshold and generating the corresponding ROC curves.

We note the following:

- All other systems parameters of interest are fixed at their default values. This will allow us to assess the effects of varying the SIFT scale threshold on the detection results.
- Since the SIFT features are only generated from video imagery, varying this parameter will affect the detection results generated from optical imagery but will not affect the results generated from LIDAR data. Hence, we only present the experimental results generated form the optical imagery.
- Since the training vocabulary depends on this parameter, a new training vocabulary is first generated for each tested value of the SIFT scale threshold and then loop detection is performed using this SIFT parameter value and its corresponding newly generated vocabulary.
- As we did for the probably threshold parameter discussed in the previous section, this experimentation analysis of this parameter was done using the 12PM and the 4PM data sets.

Table 2-3 Tested System Parameters Setting for Variable SIFT Scale Threshold

System Component	Parameter	Variability	Initial Value	Step Size	Final Value	Default Value
FAB-MAP	Probability threshold	Fixed				0.99
SIFT	SIFT scale threshold	Iterated	1.0	1	10	
VD-LSD	LSD property vector dimension	Fixed				6
	LSD property vector selected properties	Fixed				[10, 13, 14, 20, 21, 22]
	Number of quantization bins per dimension	Fixed				2
	Minimum E3/E1 ratio	Fixed				0.1

The experimental results are illustrated and discussed next.

2.3.2 Results and Discussion

Figure 2-3 and Figure 2-4 illustrate the experimental results, generated by varying the SIFT scale threshold parameter while keeping all other selected system parameters fixed, as indicated in Table 2-2, for the 12 PM and 4PM data sets, respectively. For each figure:

- The top graph shows a ROC scatter plot of the probability of detection vs. the probability of false alarm, for each tested value of the SIFT scale threshold value.
- The bottom graph illustrates the dependence of the probability of detection on the selected value of the SIFT scale threshold.

In view of these results, we make the following observations:

- The probability of false alarm is always zero for the various tested values of the SIFT scale threshold. Again, as discussed for the probability threshold, this is likely due to the fact that false FAB-MAP loop detections are rejected by 6 DOF validation post-processing operation of the ASLAM API. The image-based results are slightly better for the 12PM data set as compared to the 4PM data set. This is to be expected, as the 12PM data set was acquired under better illumination and visibility conditions.
- For both data sets, the selected default value of the SIFT scale threshold (2.0) yields the best results. Thus, it appears to be optimal, compared to the other tested values of this parameter.
- We note that, for both tested data sets, the SIFT scale threshold value of 1.0 yields detection results, which are inconsistent with the results of the other values of this parameter. The number of features generated using this parameter value was found to be too large when using the full set of training images, which posed a problem during the Chow-Liu Tree learning using the available disk space on the system. As such, we had to significantly reduce the number of training images. This may be the reason behind the inconsistent results obtained for this parameter value.

This completes the experimental analysis of the probability threshold parameter. Next, we examine the effects of varying the VD-LSD parameters.

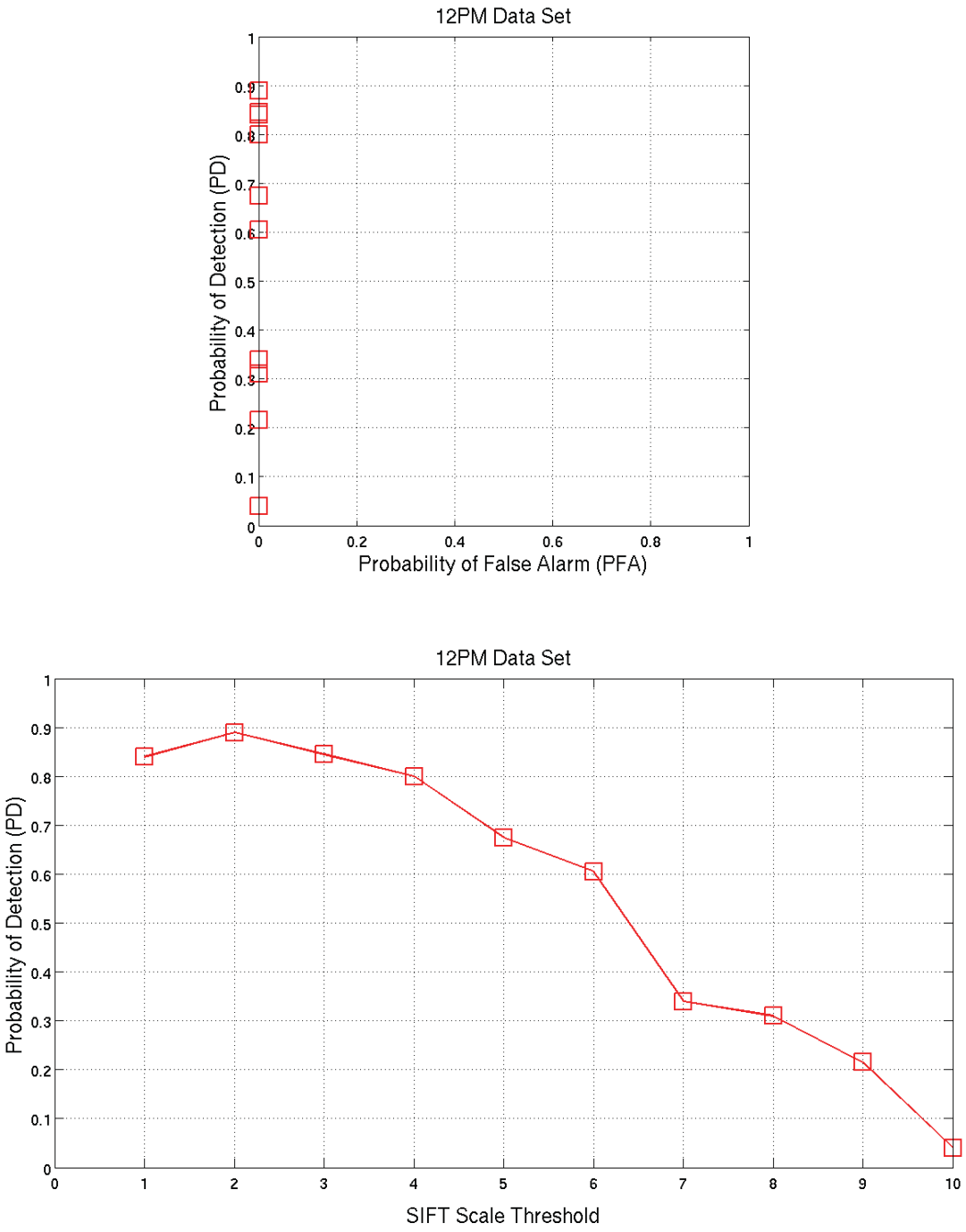

Figure 2-3 Sensitivity of the Detection Results to the Variability of the SIFT Scale Threshold for the 12PM Data Set

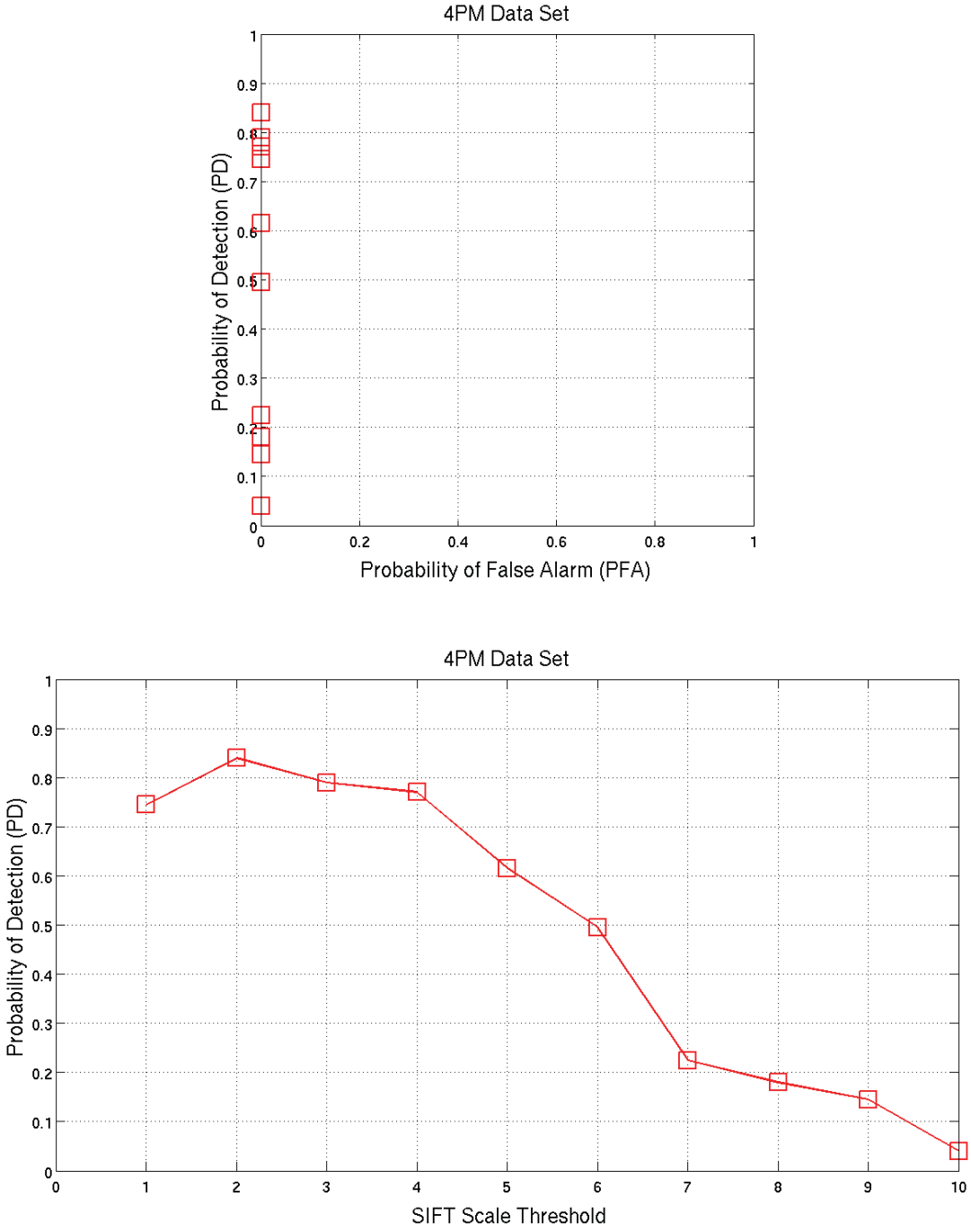

Figure 2-4 Sensitivity of the Detection Results to the Variability of the SIFT Scale Threshold for the 4PM Data Set

2.4 ROC Analysis for VD-LSD Parameters

As discussed earlier, we investigated the effects of varying the following parameters related to the selection of the VD-LSD properties:

- The dimension of the VD-LSD properties vector
- The selected properties
- The number of quantization bins for each dimension
- The minimum E3/E1 ratio.

A summary of the system parameters setting is illustrated in Table 2-4.

Table 2-4 Tested System Parameters Setting for Variable VD-LSD Parameters

System Component	Parameter	Variability	Default Value
FAB-MAP	Probability threshold	Fixed	0.99
SIFT	SIFT scale threshold	Fixed	2.0
VD-LSD	LSD property vector dimension	Iterated	
	LSD property vector selected properties	Iterated	
	Number of quantization bins per dimension	Iterated	
	Minimum E3/E1 ratio	Iterated	

Table 2-5 illustrates the list of all VD-LSD properties and their descriptions. These properties are grouped into three types [R-3] [R-4]:

- Direction properties: These properties describe the rotation that aligns the orthonormal frame of a neighbouring point with the reference frame. This rotation can be represented in various forms and therefore it is possible to construct several extended properties.
- Position properties: The coordinates of each neighbouring point expressed in the reference frame, x, y, and z along the major, semi-major and minor axis, respectively, form the three basic position properties. Several extended position properties can be calculated based on these coordinates.
- Dispersion properties: Eigenvalues of the neighbourhood covariance matrix form the three basic dispersion scalars. Three scale independent extended dispersion properties are generated by normalizing the basic values by their corresponding dispersion property of the reference point.

Table 2-5 The VD-LSD Properties

ID	Name	Description	Type
1	*prp_THETA*	A dot product of the center point's major axis and neighbourhood point's major axis.	Direction properties
2	*prp_PHI*	A dot product of the center point's minor axis and neighbourhood point's minor axis.	
3	*prp_PSI*	A dot product of the center point's minimum axis and neighbourhood point's minimum axis.	
4	*prp_ALPHA*	First ZYZ Euler Angle for center point's eigenvectors (or frame) on world frame.	
5	*prp_BETA*	Second ZYZ Euler Angle for center point's eigenvectors (or frame) on world frame.	
6	*prp_GAMMA*	Third ZYZ Euler Angle for center point's eigenvectors (or frame) on world frame.	
7	*prp_ROLL*	First ZYX Euler Angle for center point's eigenvectors (or frame) on world frame.	
8	*prp_PITCH*	Second ZYX Euler Angle for center point's eigenvectors (or frame) on world frame.	
9	*prp_YAW*	Third ZYX Euler Angle for center point's eigenvectors (or frame) on world frame.	
10	*prp_X*	X value of vector from center point to a neighbourhood point on world frame.	Position Properties
11	*prp_Y*	Y value of vector from center point to a neighbourhood point on world frame.	
12	*prp_Z,*	Z value of vector from center point to a neighbourhood point on world frame.	
13	*prp_XA*	Length of vector from center point to a neighbourhood point on world frame's Y-Z plain. Square root of (prp_Y^2 + prp_Z^2)	
14	*prp_YA*	Length of vector from center point to a neighbourhood point on world frame's X-Z plain. Square root of (prp_X^2 + prp_Z^2)	
15	*prp_ZA*	Length of vector from center point to a neighbourhood point on world frame's Y-Y plain. Square root of (prp_X^2 + prp_Y^2)	
16	*prp_POINTDIST*	Length of vector from center point to a neighbourhood point.	
17	prp_R1 (E1 / (E1 of the reference point))	First eigenvalue of center point divided by the first eigenvalue of a neighbourhood point.	Dispersion Properties
18	prp_R2 (E2 / (E2 of the reference point))	Second eigenvalue of center point divided by the second eigenvalue of a neighbourhood point.	
19	prp_R3 (E3 / (E3 of the reference point))	Third eigenvalue of center point divided by the third eigenvalue of a neighbourhood point. If the third eigenvalue of center point is less than 0.000001, set prp_R3 value to prp_R3_MAX (defined in same file.).	

ID	Name	Description	Type
20	prp_E1	First eigenvalue of center point.	
21	prp_E2	Second eigenvalue of center point.	
22	prp_E3	Third eigenvalue of center point.	
23	prp_E1_NRML (E1 / (E1+E2+E3))	First normalized eigenvalue of center point.	
24	prp_E2_NRML (E2 / (E1+E2+E3))	Second normalized eigenvalue of center point.	
25	prp_E3_NRML (E3 / (E1+E2+E3))	Third normalized eigenvalue of center point.	

We note the following:

- Since the VD-LSD properties are only generated from LIDAR data, varying this parameter will affect the detection results generated from LIDAR data but will not affect the results generated from optical imagery. Hence, we only present the experimental results generated form the LIDAR data.
- Since the training vocabulary depends on this parameter, a new training vocabulary is first generated for each tested value of the VD-LSD properties vector and number of quantization bins. Loop detection is then performed using the selected VD-LSD parameters and their corresponding newly generated vocabulary.
- This experimentation analysis of the VD-LSD parameters was done using only the 12PM data set, as LIDAR-based results should not depend of the weather and illumination conditions during data acquisitions.

Next, we examine the dependence of the loop detection results on the dimension of the VD-LSD related parameters:

1. VD-LSD vector dimension and selected properties
2. The number of quantization bins per each dimension
3. The minimum E3/E1 ratio.

Before presenting the experimental results, we make the following observations:

- When investigating the effects of VD-LSD vector dimension and selected properties, the sample space of selection is clearly quite large. For example, when selecting a 3-dimensional VD-LSD vectors. There are ${}_{25}C_3 = 2300$ ways of selecting 3-dimensional VD-LSD property vectors from the 25 possible properties listed in Table 2-5. Since, testing all such combinations is not feasible, we randomly select a small sample of 20 three-dimensional VD-LSD property vectors and generate the detection results. This selected number of vectors was not set scientifically, but it was purely set based on the available resources. Clearly, larger samples should give provide us with more insights about the sensitivity of the detection results on the selected property vectors. This is the case for all other tested VD-LSD vector dimensions.

- Also, for a selected number of quantization bins per dimensions q and VD-LSD property vector of dimension d, the resulting feature vector has q^d elements. So, clearly this exponential computational complexity between these two VD-LSD-related parameters forces us to limit their range of feasible values.
- When investigating the effects of the VD-LSD properties vector dimension and values, the minimum E3/E1 ratio VD-LSD parameter is fixed at its default value of 0.1.
- The experimental results generated for each of the above tested parameters are presented first in the next few sub-sections. These results are then compared and discussed in Section 2.4.7.

We begin by illustrating the results for the 3-dimensional VD-LSD vector selection.

2.4.1 3-Dimensional Property Vectors

As illustrated in Table 2-6, we begin by selecting 3-dimensional property vectors, which are composed of one property of each type. Table 2-7 illustrates 20 randomly selected such 3-dimensional property vectors.

Figure 2-5 illustrates the detection results, using the selected 3-dimensional property vectors at three different values of quantization bins per dimension.

Table 2-6 3-Dimensional VD-LSD Properties Selection

Type	Index Range	# Selected Properties
Direction properties	[1-9]	1
Position Properties	[10-16]	1
Dispersion Properties	[17-25]	1

Table 2-7 Randomly Selected 3-Dimensional Property Vectors

Index	Property Vector (IDs)
1	[2, 16, 21]
2	[7, 16, 19]
3	[4, 13, 23]
4	[8, 10, 18]
5	[4, 10, 21]
6	[4, 11, 18]
7	[9, 14, 21]
8	[9, 10, 23]
9	[7, 13, 18]

Index	Property Vector (IDs)
10	[6, 12, 18]
11	[2, 16, 17]
12	[2, 16, 17]
13	[1, 16, 18]
14	[1, 12, 21]
15	[8, 16, 18]
16	[9, 14, 17]
17	[8, 16, 18]
18	[9, 14, 17]
19	[8, 16, 18]
20	[9, 14, 17]

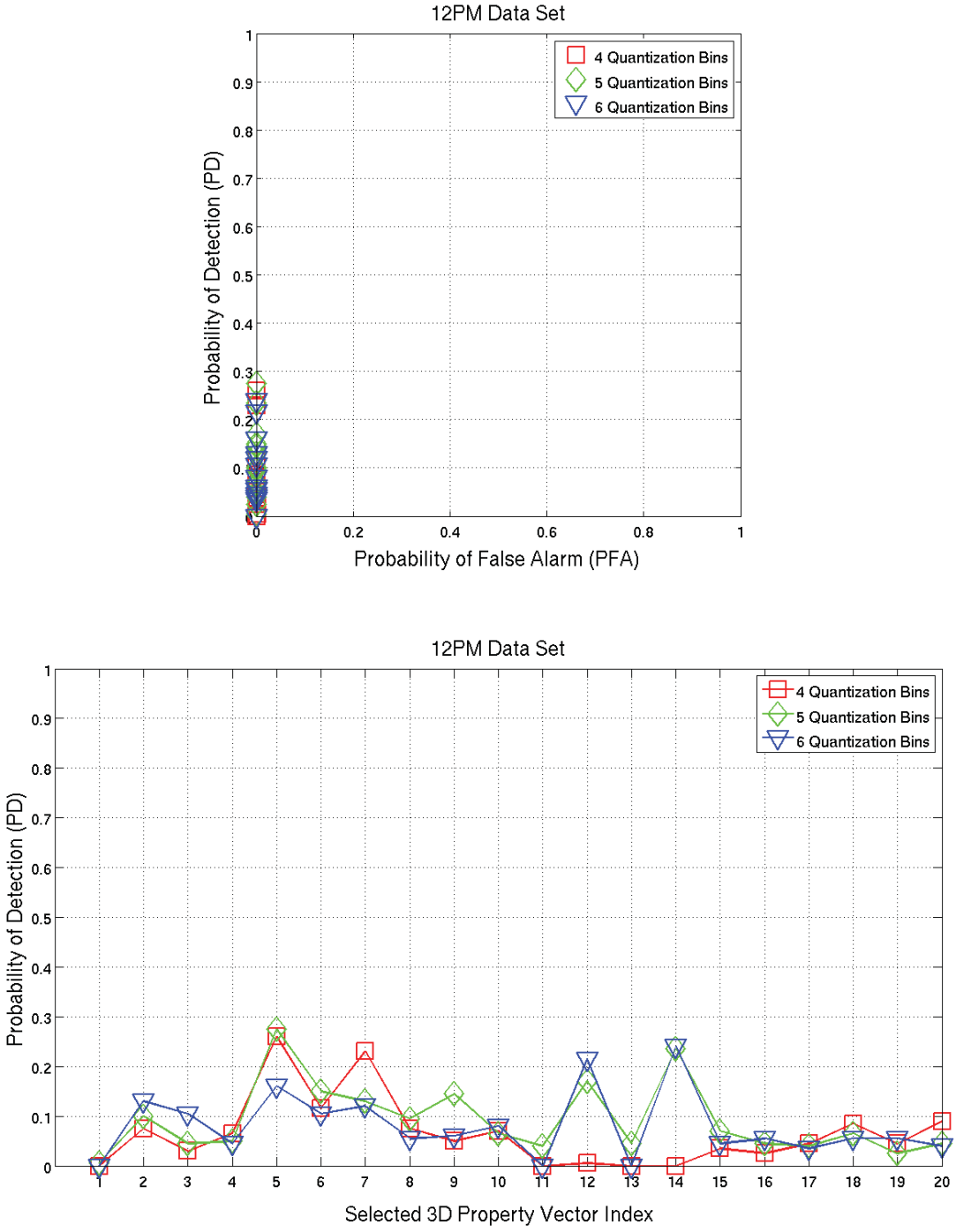

Figure 2-5 Sensitivity of the Detection Results to the Selection of the 3-Dimensional VD-LSD properties and Number of Quantization Bins per Dimension for the 12PM Data Set

Table 2-8 illustrates the best generated experimental results for the three levels of quantization bins. Note that property number 21, namely the second Eigen value of centre point (prp_E2), is a common property of these three results.

Table 2-8 Best Experimental Results for 3-Dimensional VD-LSD

# Quantization Bins	Property Vector Index	Property Vector (IDs)	Probability of Detection
4	5	[4, 10, 21]	0.260
5	5	[4, 10, 21]	0.275
6	14	[1, 12, 21]	0.240

Next, we select 4-dimensional property vectors.

2.4.2 4-Dimensional Property Vectors

As illustrated in Table 2-9, we begin by selecting 4-dimensional property vectors, which are composed of two position properties and two dispersion properties. We did not include any direction properties because previous experimentations have indicated that the position and dispersion properties may be more significant than their direction counterparts. Table 2-10 illustrates 20 randomly selected such 4-dimensional property vectors.

Figure 2-6 illustrates the detection results, using the selected 4-dimensional property vectors at two different values of quantization bins per dimension.

Table 2-9 4-Dimensional VD-LSD Properties Selection

Type	Index Range	# Selected Properties
Direction properties	[1-9]	0
Position Properties	[10-16]	2
Dispersion Properties	[17-25]	2

Table 2-10 Randomly Selected 4-Dimensional Property Vectors

Index	Property Vector (IDs)
1	[10, 14, 20, 22]
2	[10, 16, 20, 21]
3	[13, 15, 19, 24]
4	[10, 13, 18, 23]
5	[11, 13, 20, 22]
6	[11, 15, 19, 25]
7	[11, 15, 18, 19]

Index	Property Vector (IDs)
8	[10, 14, 21, 23]
9	[12, 14, 22, 23]
10	[14, 16, 18, 23]
11	[10, 11, 21, 22]
12	[13, 14, 20, 23]
13	[12, 14, 19, 24]
14	[13, 14, 19, 24]
15	[10, 12, 22, 25]
16	[13, 14, 21, 22]
17	[13, 15, 21, 25]
18	[10, 11, 17, 20]
19	[12, 13, 22, 23]
20	[15, 16, 18, 25]

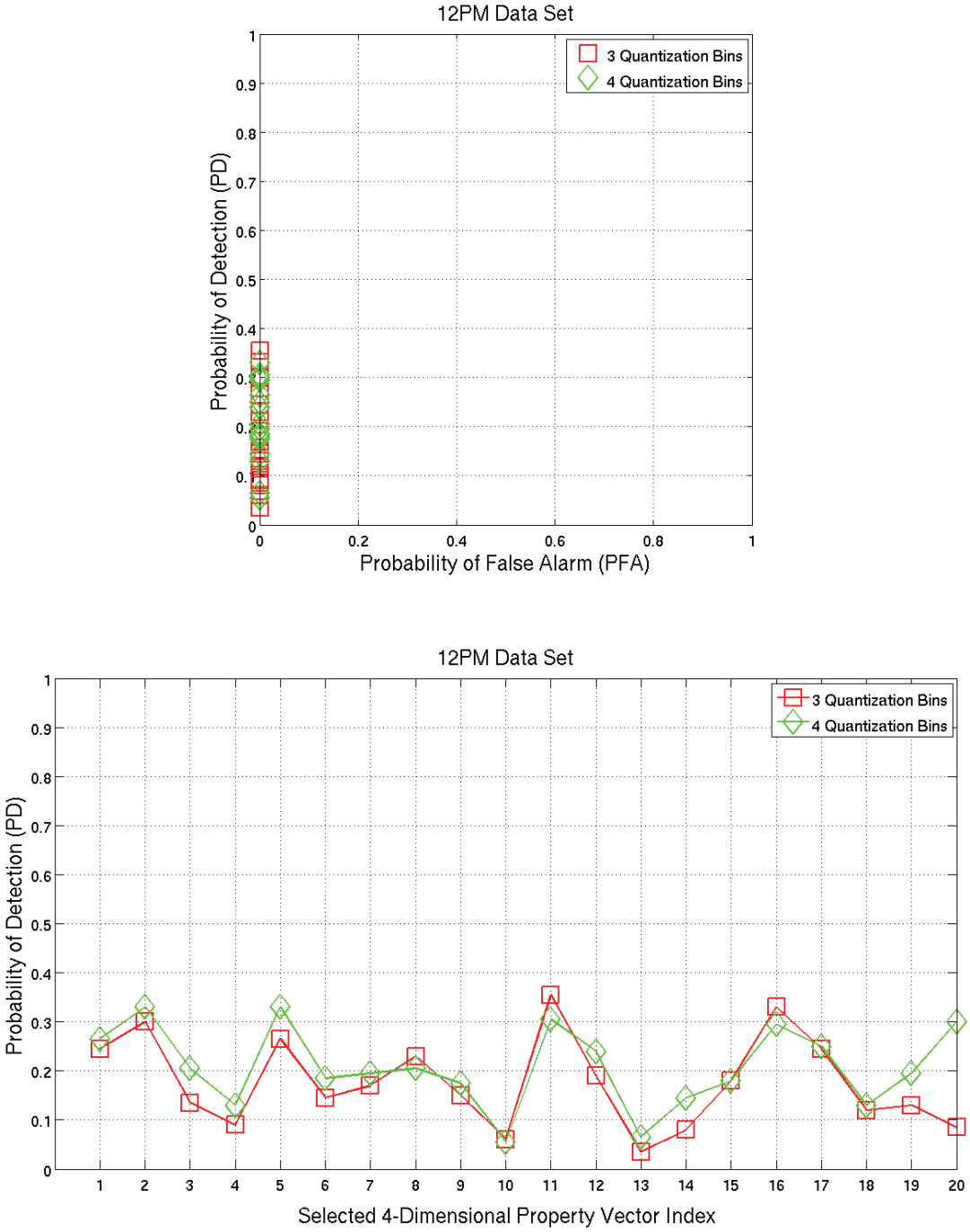

Figure 2-6 Sensitivity of the Detection Results to the Variability of the 4-Dimensional VD-LSD Properties and Number of Quantization Bins per Dimension for the 12PM Data Set

Table 2-11 illustrates the best generated experimental results for the two levels of quantization bins. Note that the same properties yield the best results for two quantization levels. Property number 21, namely the second Eigen value of centre point (prp_E2), is again one of the selected properties.

Table 2-11 Best Experimental Results for 4-Dimensional VD-LSD

# Quantization Bins	Property Vector Index	Property Vector (IDs)	Probability of Detection
3	11	[10, 11, 21, 22]	0.355
4	11	[10, 11, 21, 22]	0.305

Next, we select 5-dimensional property vectors.

2.4.3 5-Dimensional Property Vectors

As illustrated in Table 2-12, we begin by selecting 5-dimensional property vectors, which are composed of two position properties and three dispersion properties. Table 2-13 illustrates 20 randomly selected such 5-dimensional property vectors. As mentioned above, we did not include any direction properties because position and dispersion properties are believed to be more significant than their direction counterparts.

Figure 2-7 illustrates the detection results, using the selected 5-dimensional property vectors at two different values of quantization bins per dimension.

Table 2-12 5-Dimensional VD-LSD Properties Selection

Type	Index Range	# Selected Properties
Direction properties	[1-9]	0
Position Properties	[10-16]	2
Dispersion Properties	[17-25]	3

Table 2-13 Randomly Selected 5-Dimensional Property Vectors

Index	Property Vector (IDs)
1	[12, 16, 17, 19, 25]
2	[11, 11, 12, 21, 25]
3	[12, 14, 16, 22, 23]
4	[5, 11, 14, 18, 25]
5	[5, 10, 13, 23, 24]
6	[12, 13, 18, 22, 25]
7	[12, 13, 14, 18, 20]
8	[10, 14, 15, 19, 20]
9	[11, 12, 19, 21, 22]
10	[3, 15, 16, 20, 22]
11	[1, 15, 16, 19, 22]
12	[3, 11, 12, 18, 20]
13	[1, 13, 14, 22, 23]
14	[10, 11, 12, 21, 22]
15	[3, 15, 16, 19, 21]
16	[7, 14, 15, 17, 20]
17	[11, 13, 13, 21, 24]
18	[14, 16, 17, 19, 25]
19	[7, 12, 14, 17, 23]
20	[11, 14, 20, 20, 24]

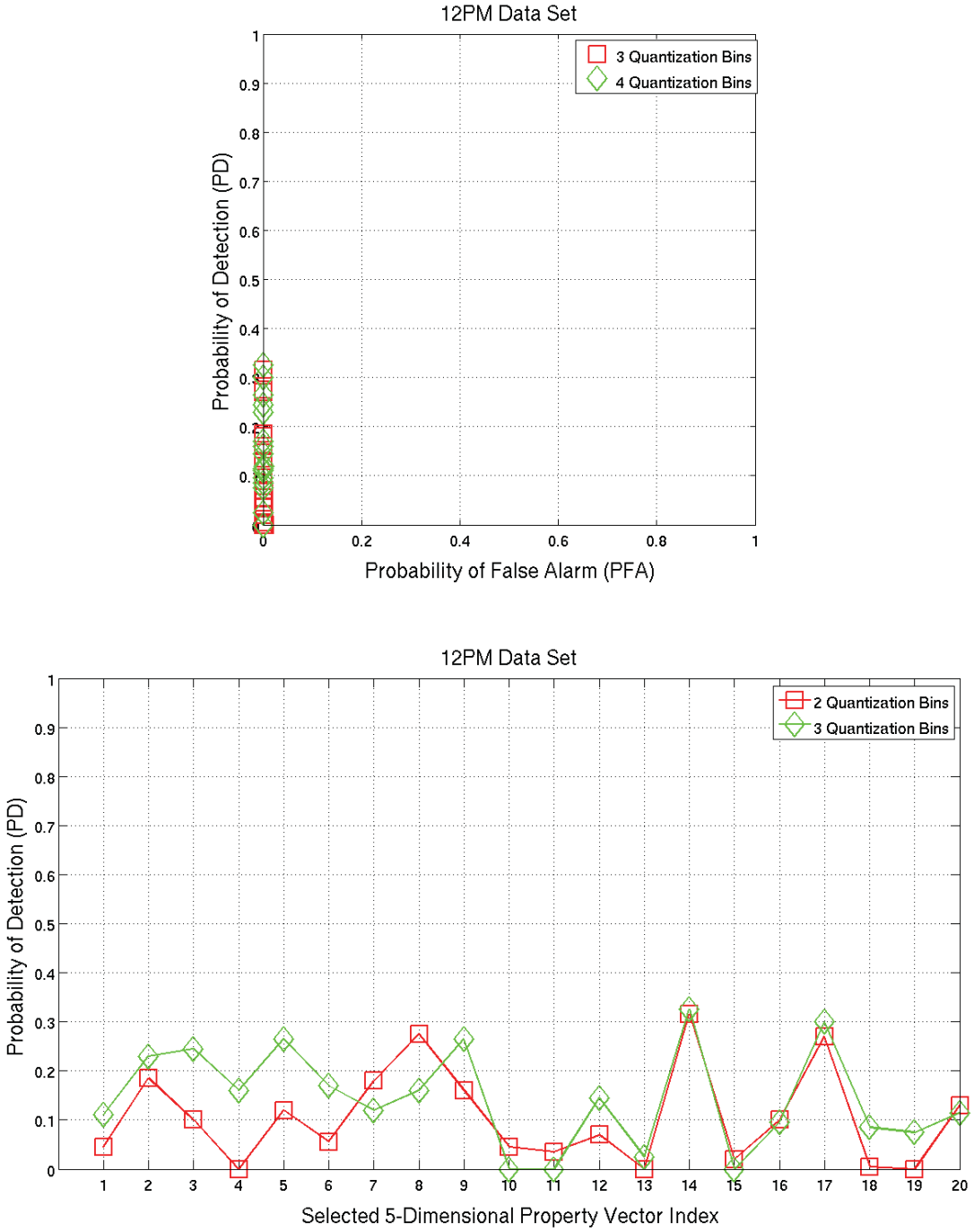

Figure 2-7 Sensitivity of the Detection Results to the Variability of the 5-Dimensional VD-LSD Properties and Number of Quantization Bins per Dimension for the 12PM Data Set

Table 2-16 illustrates the best generated experimental results for the two levels of quantization bins. Note that the same properties yield the best results for two quantization levels.

Table 2-14 Best Experimental Results for 5-Dimensional VD-LSD.

# Quantization Bins	Property Vector Index	Property Vector (IDs)	Probability of Detection
2	14	[10, 11, 12, 21, 22]	0.315
3	14	[10, 11, 12, 21, 22]	0.325

Next, we select 6-dimensional property vectors.

2.4.4 6-Dimensional Property Vectors

We explore two ways of selecting the 6-dimensional property vector. The first approach involves selecting two properties from each class of properties while the other way involves selecting three properties from the position and dispersion classes but no direction properties. These two properties selection approaches will help us to explore whether the position and dispersion properties are actually more significant than their direction counterparts.

2.4.4.1 Using Two Properties of Each Type (Approach 1)

As illustrated in Table 2-15, we begin by selecting 6-dimensional property vectors, which are composed of two direction properties, two position and two dispersion properties. Table 2-16 illustrates 20 randomly selected such 6-dimensional property vectors.

Figure 2-7 illustrates the detection results, using the selected 6-dimensional property vectors at two different values of quantization bins per dimension.

Table 2-15 6-Dimensional VD-LSD Properties Selection (Approach 1)

Type	Index Range	# Selected Properties
Direction properties	[1-9]	2
Position Properties	[10-16]	2
Dispersion Properties	[17-25]	2

Table 2-16 Randomly Selected 6-Dimensional Property Vectors (Approach 1)

Index	Property Vector (IDs)
1	[3, 5, 11, 15, 18, 19]
2	[3, 4, 12, 16, 18, 20]
3	[4, 9, 10, 11, 20, 22]
4	[3, 6, 11, 14, 18, 19]
5	[3, 4, 10, 13, 19, 24]
6	[1, 9, 13, 15, 19, 22]
7	[5, 9, 11, 13, 21, 22]
8	[4, 7, 12, 16, 17, 24]
9	[8, 9, 10, 11, 20, 23]
10	[2, 7, 10, 14, 21, 24]
11	[7, 9, 12, 16, 18, 23]
12	[1, 7, 13, 16, 22, 24]
13	[6, 8, 11, 16, 17, 21]
14	[2, 9, 13, 14, 17, 21]
15	[1, 7, 10, 13, 17, 24]
16	[7, 8, 11, 14, 21, 25],
17	[6, 8, 13, 15, 17, 18]
18	[2, 4, 10, 15, 20, 21]
19	[4, 6, 12, 14, 17, 20]
20	[2, 9, 10, 12, 18, 21]

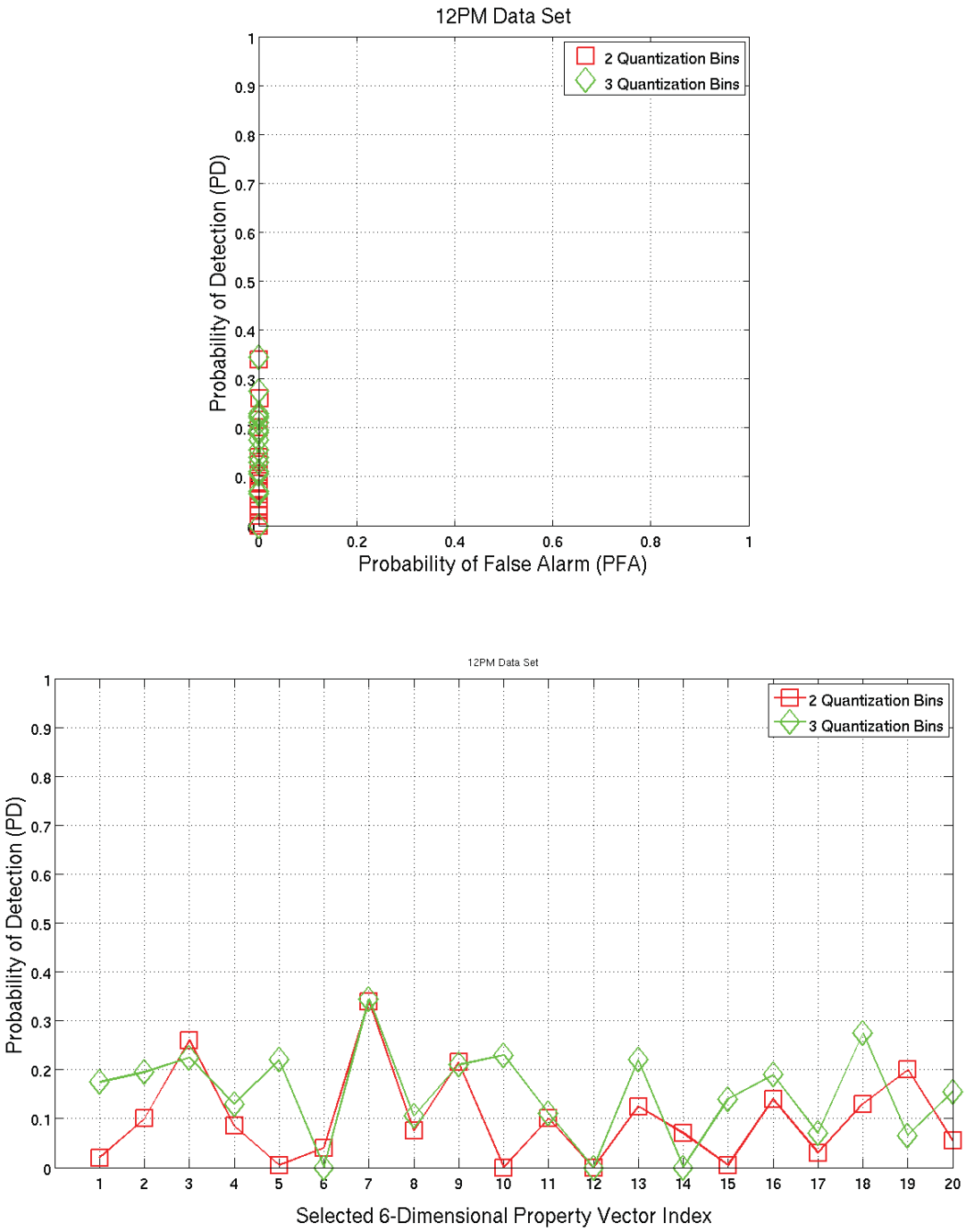

Figure 2-8 Sensitivity of the Detection Results to the Variability of the 6-Dimensional VD-LSD Properties and Number of Quantization Bins per Dimension for the 12PM Data Set (Approach 1)

Table 2-17 illustrates the best generated experimental results for the two levels of quantization bins. Note that the same properties yield the best results for two quantization levels.

Table 2-17 Best Experimental Results for 6-Dimensional VD-LSD (Approach 1)

# Quantization Bins	Property Vector Index	Property Vector (IDs)	Probability of Detection
2	7	[5, 9, 11, 13, 21, 22]	0.340
3	7	[5, 9, 11, 13, 21, 22]	0.345

Next, we illustrate the results when the 6-dimensional property vectors are composed of only position and dispersion properties.

2.4.4.2 Using Position and Dispersion Properties Only (Approach 2)

As illustrated in Table 2-18, we begin by selecting 6-dimensional property vectors, which are composed of three direction properties and three position properties. Table 2-19 illustrates 21 randomly selected such 6-dimensional property vectors. The first property vector is set to the default 6-dimensional property vector.

Figure 2-9 illustrates the detection results, using the selected 6-dimensional property vectors at two different number of quantization bins per dimension.

Table 2-18 6-Dimensional VD-LSD Properties Selection (Approach 2)

Type	Index Range	# Selected Properties
Direction properties	[1-9]	0
Position Properties	[10-16]	3
Dispersion Properties	[17-25]	3

Table 2-19 Randomly Selected 6-Dimensional Property Vectors (Approach 2)

Index	Property Vector (IDs)
1	[10, 13, 14, 20, 21, 22] (Default value)
2	[11, 12, 16, 19, 21, 22]
3	[12, 14, 15, 19, 21, 25]
4	[12, 13, 15, 17, 21, 24]
5	[10, 13, 16, 17, 20, 21]
6	[11, 12, 15, 18, 21, 22]
7	[11, 14, 15, 17, 19, 21]
8	[11, 15, 16, 17, 21, 25]
9	[10, 13, 16, 17, 23, 24]
10	[10, 12, 16, 19, 20, 24]
11	[10, 11, 16, 21, 22, 24]
12	[11, 14, 15, 17, 20, 21]
13	[10, 11, 12, 17, 21, 25]
14	[12, 13, 16, 18, 20, 24]
15	[10, 11, 12, 18, 22, 25]
16	[10, 11, 12, 17, 18, 24]
17	[13, 14, 15, 19, 21, 23]
18	[11, 12, 14, 17, 22, 24]
19	[13, 15, 16, 19, 20, 21]
20	[13, 14, 15, 20, 21, 24]
21	[12, 13, 16, 18, 19, 22]

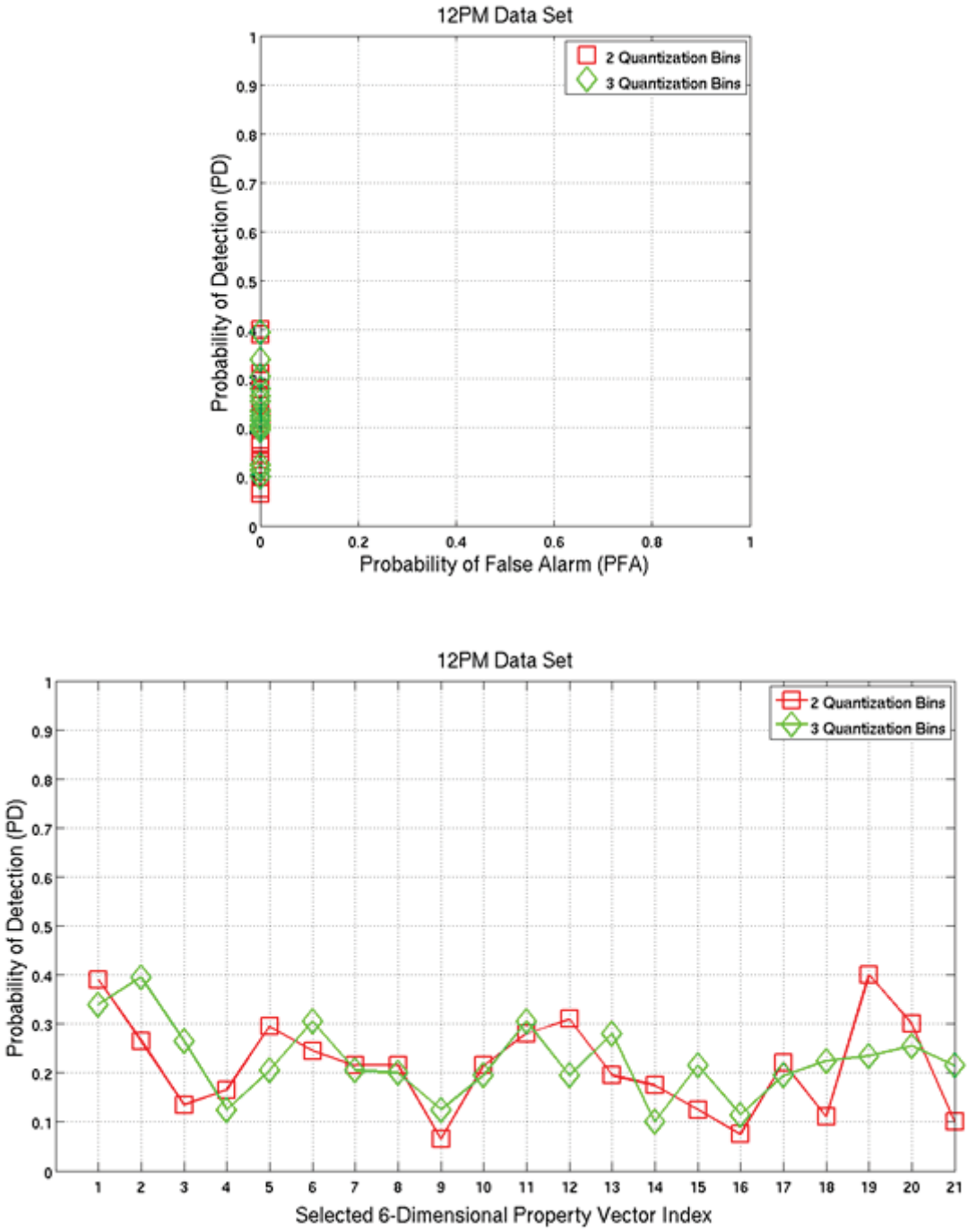

Figure 2-9 Sensitivity of the Detection Results to the Variability of the 6-Dimensional VD-LSD Properties and Number of Quantization Bins per Dimension for the 12PM Data Set (Approach 2)

Table 2-20 illustrates the best generated experimental results for the two levels of quantization bins.

Table 2-20 Best Experimental Results for 6-Dimensional VD-LSD (Approach 2).

# Quantization Bins	Property Vector Index	Property Vector (IDs)	Probability of Detection
2	19	[13, 15, 16, 19, 20, 21]	0.400
3	2	[11, 12, 16, 19, 21, 22]	0.395

Next, we select 7-dimensional property vectors.

2.4.5 7-Dimensional Property Vectors

As illustrated in Table 2-21, we begin by selecting 7-dimensional property vectors, which are composed of three direction properties and three position properties plus an additional property, which can be any one of the remaining 19 properties. Table 2-22 illustrates 20 randomly selected such 7-dimensional property vectors.

Figure 2-10 illustrates the detection results, using the selected 7-dimensional property vectors at two quantization bins per dimension.

Table 2-21 7-Dimensional VD-LSD Properties Selection

Type	Index Range	# Selected Properties
Direction properties	[1-9]	0
Position Properties	[10-16]	3
Dispersion Properties	[17-25]	3
All properties	[1-25]	1

Table 2-22 Randomly Selected 7-Dimensional Property Vectors

Index	Property Vector (IDs)
1	[7, 13, 14, 15, 18, 20, 22]
2	[9, 10, 11, 15, 17, 20, 23]
3	[10, 11, 12, 15, 20, 23, 24]
4	[11, 12, 15, 17, 19, 24, 25]
5	[11, 13, 15, 21, 23, 24, 25]
6	[11, 12, 14, 14, 19, 23, 24]
7	[10, 13, 14, 17, 18, 21, 22]
8	[1, 13, 14, 16, 22, 24, 25]
9	[13, 13, 14, 16, 19, 21, 24]
10	[14, 15, 16, 17, 19, 22, 23]
11	[10, 14, 15, 22, 23, 24, 25]
12	[10, 14, 14, 16, 18, 21, 24]
13	[4, 10, 12, 14, 17, 18, 21]
14	[10, 11, 13, 14, 19, 21, 23]
15	[10, 13, 15, 15, 18, 19, 24]
16	[5, 11, 12, 14, 17, 18, 25]
17	[10, 14, 16, 17, 23, 24, 24]
18	[13, 15, 16, 17, 18, 20, 24]
19	[12, 13, 14, 17, 22, 22, 24]
20	[10, 12, 13, 18, 19, 22, 23]

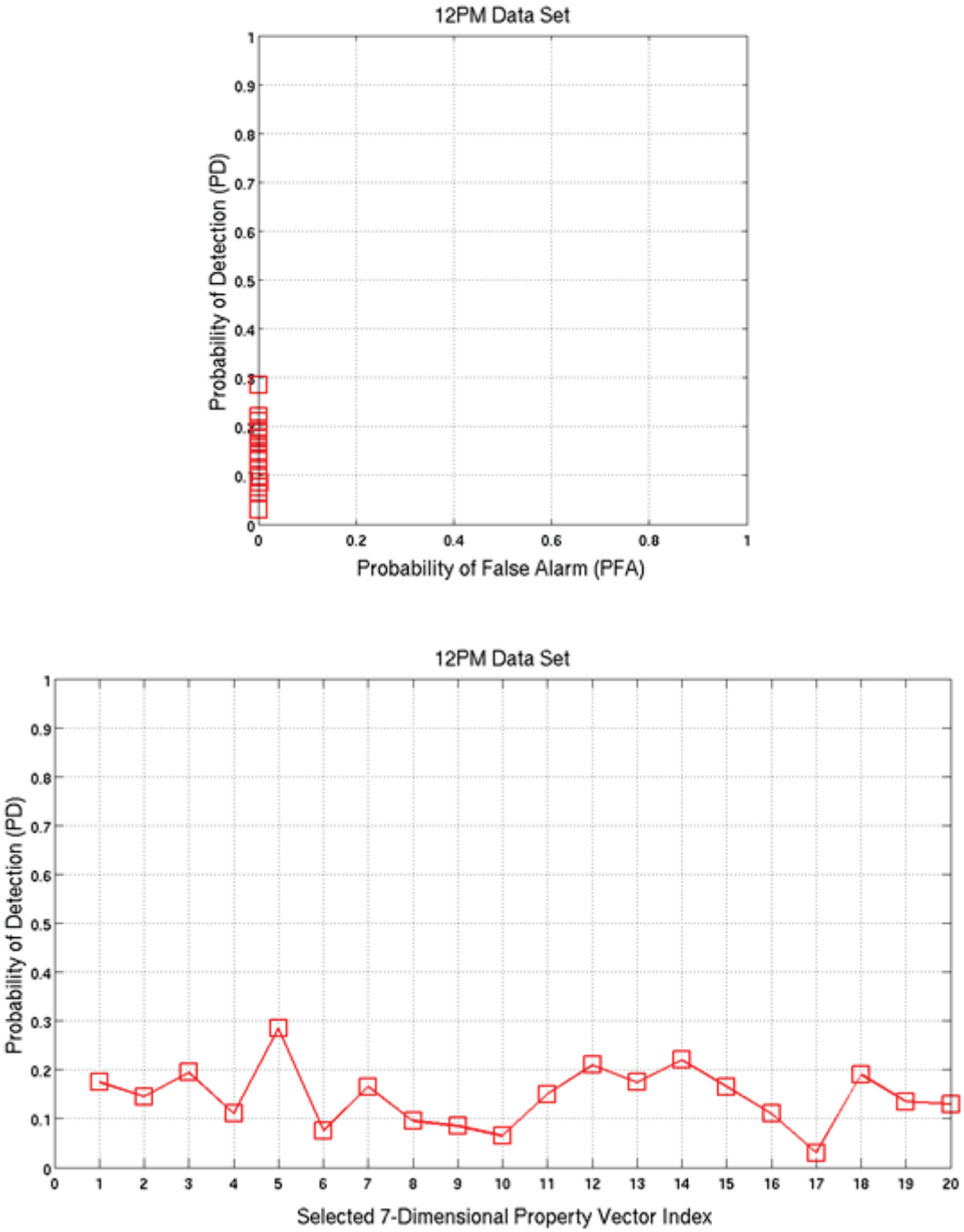

Figure 2-10 Sensitivity of the Detection Results to the Variability of the 7-Dimensional VD-LSD Properties and Number of Quantization Bins per Dimension for the 12PM Data Set using 2 Quantization Bins

Table 2-20 illustrates the best generated experimental results for two quantization bins.

Table 2-23 Best Experimental Results for 7-Dimensional VD-LSD

# Quantization Bins	Property Vector Index	Property Vector (IDs)	Probability of Detection
2	5	[11, 13, 15, 21, 23, 24, 25]	0.285

Next, we illustrate the results for variable E3/E1 ratio threshold.

2.4.6 Minimum E3/E1 Ratio Threshold

As mentioned in the previous section, the default value of the minimum E3/E1 ratio threshold has been set to 0.1. In this section, we vary this parameter, while keeping all other system settings fixed, in order to examine the sensitivity of the scene detection results to the variation of this parameter and perhaps identify a more optimal default value for this parameter.

2.4.6.1 Parameters Setting

Table 2-24 illustrates the setting of the systems parameters for examining the sensitivity of the detection results to the variability of minimum E3/E1 ratio threshold and generating the corresponding ROC curves. Note that all other systems parameters of interest are fixed at their default values. This will allow us to assess the effects of varying minimum E3/E1 ratio threshold on the detection results.

Table 2-24 Tested System Parameters Settings for Variable Minimum E3/E1 Ratio Threshold

System Component	Parameter	Variability	Initial Value	Step Size	Final Value	Default Value
FAB-MAP	Probability threshold	Fixed				0.99
SIFT	SIFT scale threshold	Fixed				2
VD-LSD	LSD property vector dimension	Fixed				6
	LSD property vector selected properties	Fixed				[10, 13, 14, 20, 21, 22]
	Number of quantization bins per dimension	Fixed				2
	Minimum E3/E1 ratio	Iterated	0.01	0.01	0.20	

Figure 2-11 illustrates the experimental results generated by varying the minimum E3/E1 ratio over the [0.01, 0.2] feasible range.

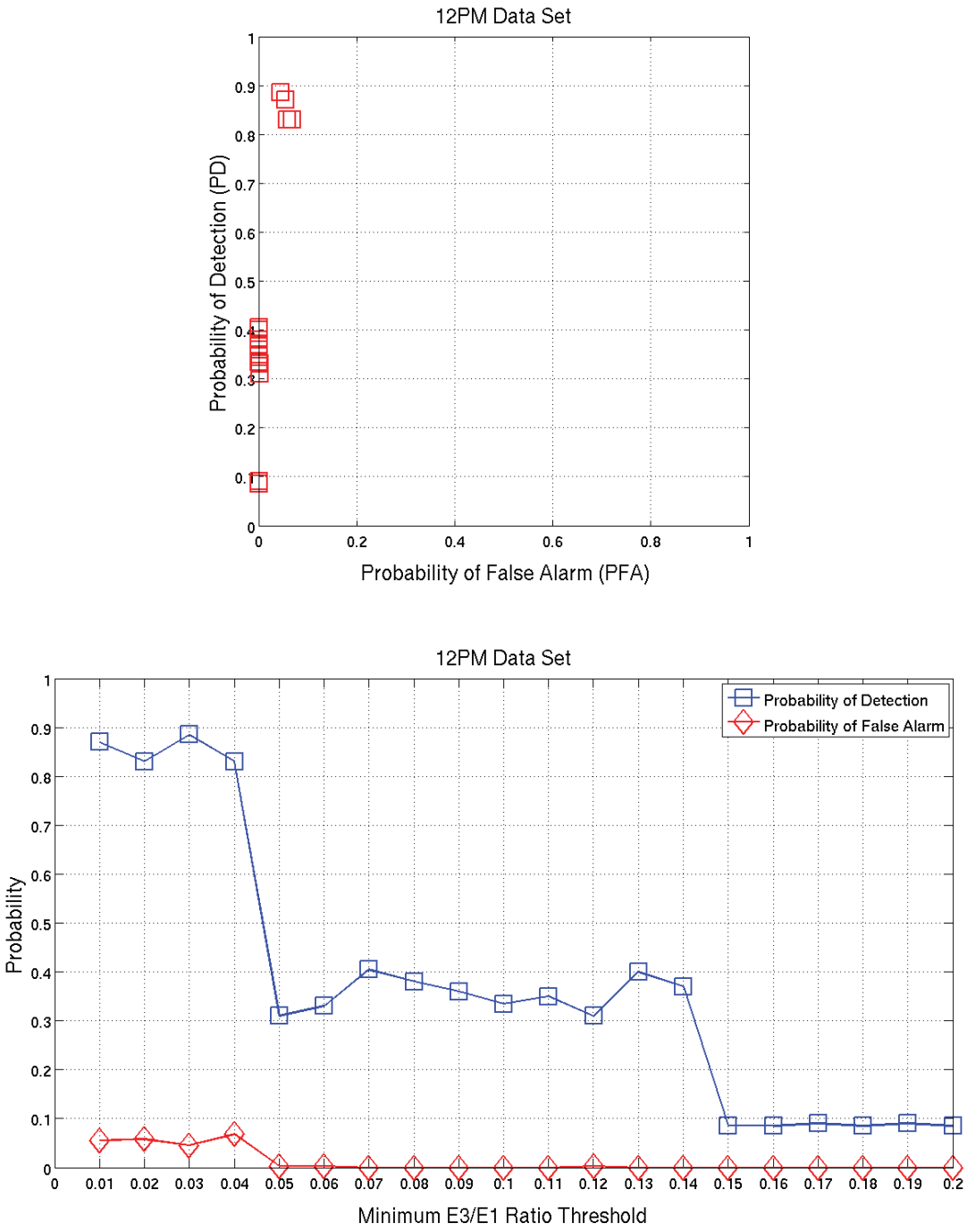

Figure 2-11 Sensitivity of the Detection Results to the Variability of the Minimum E3/E1 Ratio Threshold over the [0.01, 0.2] Range, for the 12PM Data Set

Next, we discuss the generated experimental results related to iterating the various VD-LSD parameters.

2.4.7 Discussions of the VD-LSD Experimental Results

Clearly, the detection results are significantly sensitive the selected VD-LSD properties vector. As such, we notice significant variability of the detection results using different property vectors for fixed vector dimension and quantization number of bins and other system parameters. Hence, among the 25 possible properties, some of these properties are more effective in increasing the scene detection rate than others. Clearly, in order to identify the best set of parameters to use, an exhaustive testing process is needed. This process involves testing all possible combinations of VD-LSD property vectors for each dimension and number of quantization bins. However, such as a costly process in not feasible due to the huge number of possible tests and the limited resources.

In this experimental study, we conducted a limited number of experimental tests. For each tested VD-LSD dimension, we randomly selected 20 possible VD-LSD property vectors and generate the detection results at a few different levels of quantization bins. However, as we discuss next, even though this experimental study is far from complete or comprehensive, it has provided us with some important insights about some of the important VD-LSD properties.

In an effort to identify some of the key VD-LSD properties, which appear to have significant effects on the detection results, we identified the best detection results obtained from each of the conducted tests. Table 2-25 summarizes these best experimental results and Table 2-26 illustrates the results obtained using the default VD-LSD settings, for comparison purposes. The best experimental results are also illustrated graphically in Figure 2-12 and Figure 2-13.

Table 2-25 Best Experimental Results for the Different VD-LSD Vector Dimensions and Number of Quantization Bins

VD-LSD Vector Dimension	No. Quantization Bins	Property Vector (IDs)	Probability of Detection
3	4	[4, 10, 21]	0.260
	5	[4, 10, 21]	0.275
	6	[1, 12, 21]	0.240
4	3	[10, 11, 21, 22]	0.355
	4	[10, 11, 21, 22]	0.305
5	2	[10, 11, 12, 21, 22]	0.315
	3	[10, 11, 12, 21, 22]	0.325
6 (2 of each type of properties)	2	[5, 9, 11, 13, 21, 22]	0.340
	3	[5, 9, 11, 13, 21, 22]	0.345
6 (3 position + 3 dispersion properties)	2	[13, 15, 16, 19, 20, 21]	0.400
	3	[11, 12, 16, 19, 21, 22]	0.395
7	2	[11, 13, 15, 21, 23, 24, 25]	0.285

Table 2-26 Default VD-LSD Parameters Setting

VD-LSD Vector Dimension	No. Quantization Bins	Property Vector (IDs)	Probability of Detection
6	2	[10, 13, 14, 20, 21, 22]	0.390

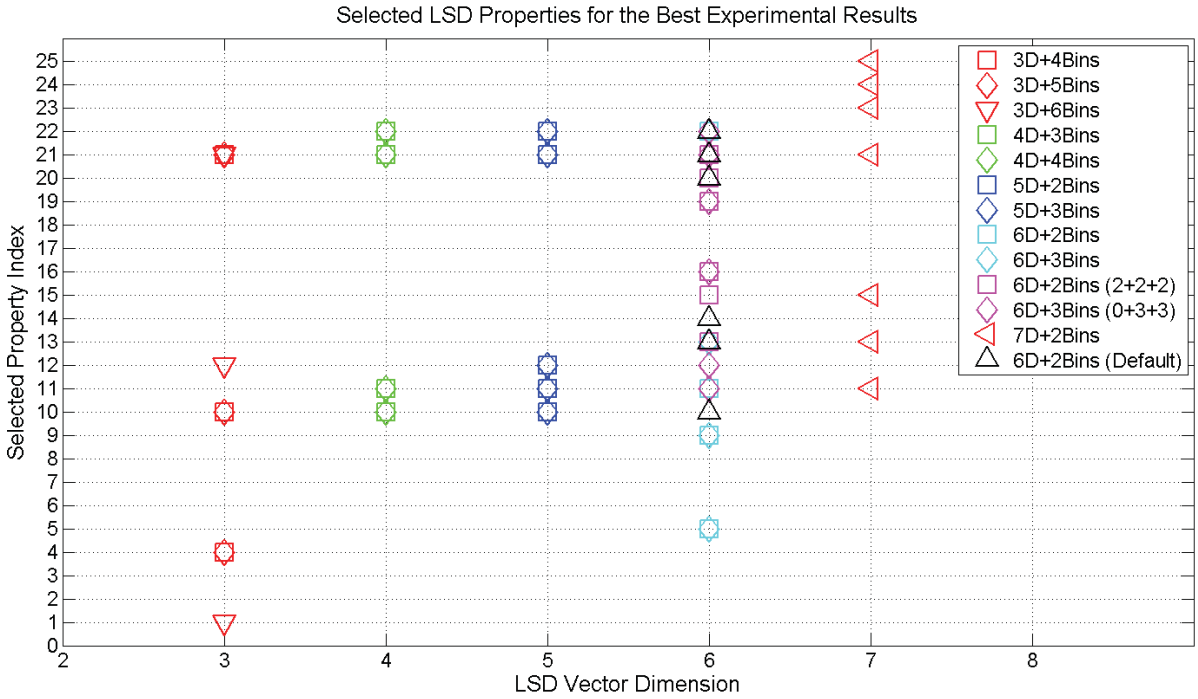

Figure 2-12 The Selected Properties for the Best Experimental Results for the Different VD-LSD Vector Dimensions and Number of Quantization Bins

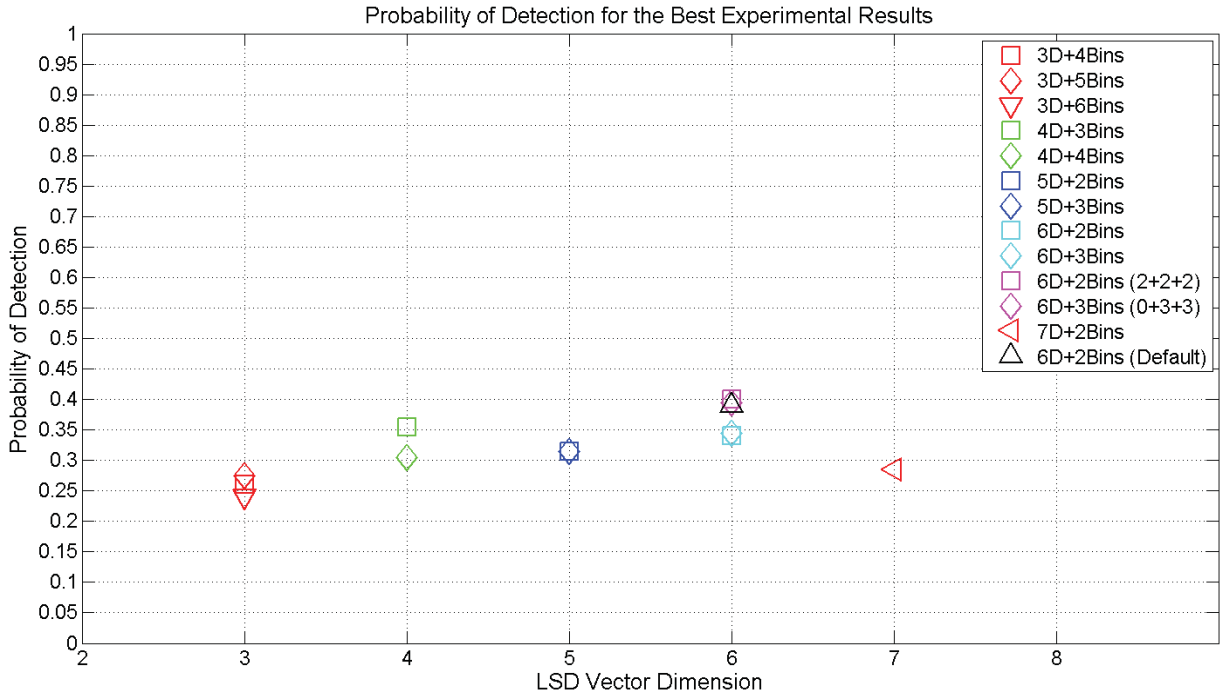

Figure 2-13 The Probability of Detection for the Best Experimental Results for the Different VD-LSD Vector Dimensions and Number of Quantization Bins

In view of these results, we observe that there are certain set of properties, which consistently appear with the elements of the VD-LSD properties vector, yielding the best experimental results. These properties are summarized in Table 2-27. We note these favorable VD-LSD properties consists of two position properties and three dispersion properties but no direction properties have been consistently selected for the different best case scenarios. This appears to indicate that the inclusion of the position and dispersion-related properties in the selected VD-LSD vectors is more important that the direction properties.

Table 2-27 Common VD-LSD Properties Yielding the Best Experimental Results

Index	Name	Description	Type
10	*prp_X*	X value of vector from center point to a neighbourhood point on world frame.	Position Properties
11	*prp_Y*	Y value of vector from center point to a neighbourhood point on world frame.	
13	*prp_XA*	Length of vector from center point to a neighbourhood point on world frame's Y-Z plain. Square root of (prp_Y^2 + prp_Z^2)	
20	prp_E1	First eigenvalue of center point.	Dispersion Properties
21	prp_E2	Second eigenvalue of center point.	
22	prp_E3	Third eigenvalue of center point.	

Let us examine the experimental results for the 6-dimensional VD-LSD vectors, using the two properties selection approaches described in sections 2.4.4.1 and 2.4.4.2. The main difference between these two approaches is that for the first approach, we treat the three types of properties as equally important and select two of each type, while for the second approach, we select three position and three dispersion properties but no direction properties. Clearly, we get better optimal results using the second properties section approach instead of the first one. This indicates, and supports previous experimental observations, that the position and dispersion properties may actually be more significant than their direction counterparts.

When it comes to the number of quantization (histogram) bins for each dimension, the experimental results appear to be somewhat inconsistent. In general, increasing the number of bins results in a higher-dimensional feature vector, with a more spread-out distribution. In many cases, this produces better detection results but this is not always the case. From Table 2-25, we observe that the best results for the different number of bins are obtained using the same selected VD-LSD property vector and the probability of detection is comparable for the different bin sizes. In fact, in some cases, we obtain better probability of detection using the lower bin size than when using the higher bin size. However, as illustrated in Figure 2-14, the computational cost increases significantly when increasing the number of histogram quantization bins from 2 to 3 bins. Given the comparable detection results and significant increase in computational complexity, it appears to be better to keep the default setting of 2 histogram quantization bins.

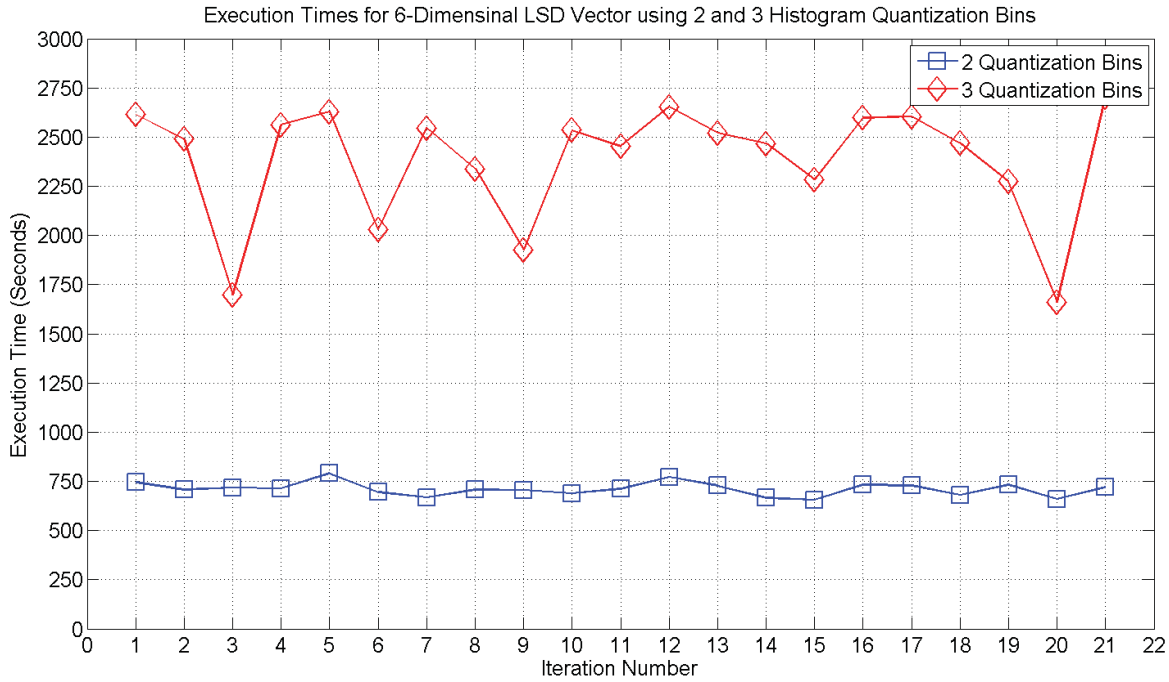

Figure 2-14 Execution Times (Including Vocabulary Generation) for the 6-Dimensional VD-LSD Vector using 2 and 3 Histogram Quantization Bins (on the ASLAM Linux Server Machine)

Clearly, increasing the dimensionality of the VD-LSD property vector generally yields better detection results. This is the case as we increase the dimensionality from 3 to 6. However, the best result obtained for the 7-dimensional VD-LSD vector does not follow this trend and it is actually worse than the results obtained for the 6-dimensinal VD-LSD vectors. However, this is likely due to the very small sample of selected VD-LSD vector for the 7-dimensional case. For this case, there ${}_{25}C_7 = 480700$ possible such 7-dimensional VD-LSD vectors. Our random sample consists of 20 such vectors, which is too small, and perhaps, by chance the selected vectors did not include some of the favourable properties. However, even if we may obtain better results for the 7-dimensional case as compared to the 6-dimensional case, this will come at an increase in computation complexity, as the feature vector dimensionality increase from $2^6 = 64$ to $2^7 = 128$. Hence, in view of the generated experimental results, we recommend to keep the default settings of using 6-dimensional VD-LSD property vectors.

The minimum E3/E1 ratio threshold appears to be such a critical VD-LSD-based system parameter. As illustrated in Figure 2-11, the detection results are quite sensitive to the variation of this parameter. Setting this parameter too low (value ≤ 0.04) results in a surprisingly high probability of detection (~ 0.80). However, this comes at the expense of some non-negligible probability of false alarm (~ 0.08). As the value of the minimum E3/E1 ratio threshold increases beyond 0.05, the probability of detection decreases significantly while the probability of false detection becomes zero. By default, this parameter has been set to 0.1. This default setting is acceptable if one has zero tolerance for false alarms, although a value of 0.07 appears to yield slightly better detection results and still no false alarms. If one allows for small tolerance (~0.05) of false alarms, setting this parameter to 0.03 yields a probability of detection of almost 0.90, which is considered a high detection rate based on LIDAR data only.

Finally, as we observed for the probability and SIFT scale threshold analysis, the probability of false alarm is almost always equal to zero, except for low values of the minimum E3/E1 ratio threshold. Again, this is likely due to the fact that ASLAM API 6 DOF validation post-processing operation rejects most, if not all, of the false FAB-MAP loop detections, which are false alarms. During visualization of the detection results, green dot are often generated, indicating FAB-MAP loop detections, which were rejected by the ASLAM API 6 DOF validation post-processing operation.

This completes the discussion of VD-LSD-related experimental results. Summary and concluding remarks are presented next.

THIS PAGE INTENTIONALLY LEFT BLANK

3 CONCLUSIONS

3.1 Summary

This report documents the conducted experimental performance evaluation of the ASLAM scene detection system. In particular, we investigated the sensitivity the detected results to the variations of a selected set of ASLAM system parameters. The selected parameters were previously set according to their default settings based on an initial basic level of experimentation. In this study, we conducted a more detailed level of experimentation, where each parameter of interest was varied over a feasible range to assess the effects on the detection results.

This experimental evaluation may be considered comprehensive for some of the selected parameters, such as the FAB-MAP engine probability threshold and the SIFT scale threshold. Each of these parameters was varied over a complete range of feasible values, while keeping all other system settings fixed, and a complete understanding of the sensitivity of the detection results to these variations was inferred from the generated experimental results.

However, for the VD-LSD-related parameters, the experimental study cannot be considered comprehensive due to the significantly large size of the feasible sets for some of these parameters. In particular, for the selected VD-LSD properties vector, the choices are too many to be tested in full. As such, for a vector dimension k, there are ${}_{25}C_k$ possible VD-LSD property vectors.

Since testing all such combinations is not feasible, we limited our experimental study to randomly select a small sample of 20 VD-LSD property vectors, for various values of vector dimensions and number of histogram bins, and generated the detection results. We have found that, although this limited experimental study is far from complete or comprehensive, it has provided us with some important insights about some of the important VD-LSD properties. As such, we were able to identify a set of VD-LSD properties, which consistently yields better detection results than others.

Finally, for the all the examined system parameters, the probability of false alarm is almost always equal to zero. As explained earlier, this is likely due to the fact that ASLAM API 6 DOF validation post-processing operation rejects most, if not all, of the false FAB-MAP loop detections, which are false alarms. This shows the advantage of the ASLAM API 6 DOF validation post-processing operation, which has been developed as part of this project.

Next, we present the recommended ASLAM system settings based on the completed experimental study.

3.2 Recommendations

Table 3-1 illustrates our recommendations for the tested ASLAM system parameters and settings based on the generated experimental results.

Table 3-1 Recommended Tested ASLAM System Parameters Settings

System Component	Parameter	Default Value	Recommendations	Comments
FAB-MAP	Probability threshold	0.99	0.95	Using the recommended value instead of the default value of this parameter, while keeping all other system parameters at their default values, increases the probability of detection from 0.90 to 0.93 (with no false alarms) for the image-only results.
SIFT	SIFT scale threshold	2.0	2.0	The default value yields the best detection results for the two analyzed test data sets.
VD-LSD	LSD property vector dimension	6	6	Dimensions higher than 6 should yield marginally better results at the expense of an increase in computational complexity. A dimension of 6 yields a good trade-off between the detection results and computational costs.
	LSD property vector selected properties	[10, 13, 14, 20, 21, 22]	[10, 11, 13, 20, 21, 22]	Using the recommended 6-D VD-LSD property vector instead of the default vector, while keeping all other system parameters at their default values, increases the probability of detection from 0.390 to 0.425 (with no false alarms) for the LIDAR-only results.
	Number of quantization bins per dimension	2	2	Given the comparable detection results for 2 or 3 quantization bins, and the significant increase in computational complexity for higher number of bins, it appears to be better to keep the default setting of 2 histogram quantization bins.

System Component	Parameter	Default Value	Recommendations	Comments
	Minimum E3/E1 ratio	0.1	0.07 (no false alarms and 0.4 PD) 0.03 (~0.05 PFA and ~0.90 PD)	A value of 0.07 appears to yield slightly better detection results and still no false alarms. If one can allow for small tolerance (~0.05) of false alarms, setting this parameter to 0.03 yields a probability of detection of almost 0.90, which is considered a high detection rate based on LIDAR data only. These results are based on the assumption that all other system parameters are fixed at their default settings.

Finally, suggestions to improve upon this completed performance evaluation experimental study are presented next.

3.3 Future Work

As mentioned previously, the conducted experimental investigation into the sensitivity of the detection results to the VD-LSD parameters was limited in scope due to the large size of the feasible regions for some of these parameters. In spite of their limited scope and size, the generated experimental results have provided us with valuable insights about the significance of some of the VD-LSD properties and identified a set of key parameters which consistently yielded better detection results than others. The conducted experimental investigation into the significance of the VD-LSD parameters can be improved by expanding its size and scope. As such, one may generate and test a much larger random sample of VD-LSD vectors. This has the potential of identifying additional properties, which tend to yield better results. Further experimental and analytical investigation of the few properties, which were found to be more significant than others, may provide us with further understanding of why they are important. This may help identify other significant properties or eliminate insignificant ones. As such, we can develop a practical heuristic methodology, which can be used as a guideline to reduce the size of the feasible region of these parameters. This will help us conduct a more comprehensive experimental performance evaluation study of the effects of the VD-LSD parameters.

In this experimental study, when evaluating the sensitivity of the detection results to a system parameter of interest, all other system parameters and settings are fixed at their default values. As such, the generated relationship between the detection results and the selected system parameter only holds for the default system settings of all other system parameters. This does not provide us with any insights into the interaction between the different system parameters. A more comprehensive study would vary more than one system variable at a time and generate relationships of the detection results on a system parameter of interest at different system settings besides the default one. This is important because one may identify a more optimized value of a system parameter of interest when changing some of the other system parameters from their default values.

The detection results for optical imagery depend on the quality of the imagery data, which in turn depends on various data acquisition parameters such as weather, visibility and illumination conditions. The current study only used datasets from a rural environment. Detection results, for both optical and LIDAR data, may vary with the type of the travelled and imaged trajectory. An imaged trajectory in an urban area may contain many features, such as buildings and traffic signs, which may appear similar, but they are not the same. On the other hand, in a rural area, the landmarks are more distinguishable. Thus it is important to investigate how the "best" system settings vary from one type of scene to another.

4 REFERENCES

R-1 Appearance Based SLAM Contract, W7702-115043/001/EDM, PWGSC, October 2010.

R-2 S. Se, ASLAM Final Report (Task 4.3), ASLAM-RP-53-4753, March 2013.

R-3 T. Pan, LSD Library Guides for ASLAM Project, TN-RD-2011-002, Issue 1.1, June 2, 2011.

R-4 B. Taati and M. Greenspan, Satellite Pose Acquisition and Tracking with Variable Dimensional Local Shape Descriptors, IEEE/RSJ IROS Workshop on Robot Vision for Space Applications, Edmonton, Canada, 5 Aug. 2005, pp 4-9.

THIS PAGE INTENTIONALLY LEFT BLANK

DOCUMENT CONTROL DATA

(Security markings for the title, abstract and indexing annotation must be entered when the document is Classified or Designated)

1. ORIGINATOR (The name and address of the organization preparing the document. Organizations for whom the document was prepared, e.g. Centre sponsoring a contractor's report, or tasking agency, are entered in section 8.)

Mohsen Ghazel; Stephen Se
MDA
13800 Commerce Parkway
Richmond, B.C.
Canada
V6V 2J3

2a. SECURITY MARKING (Overall security marking of the document including special supplemental markings if applicable.)

UNCLASSIFIED

2b. CONTROLLED GOODS

(NON-CONTROLLED GOODS)
DMC A
REVIEW: GCEC JUNE 2010

3. TITLE (The complete document title as indicated on the title page. Its classification should be indicated by the appropriate abbreviation (S, C or U) in parentheses after the title.)

ASLAM ROC Analysis Report

4. AUTHORS (last name, followed by initials – ranks, titles, etc. not to be used)

Ghazel, M.; Se, S.

5. DATE OF PUBLICATION (Month and year of publication of document.)	6a. NO. OF PAGES (Total containing information, including Annexes, Appendices, etc.)	6b. NO. OF REFS (Total cited in document.)
March 2013	70	4

7. DESCRIPTIVE NOTES (The category of the document, e.g. technical report, technical note or memorandum. If appropriate, enter the type of report, e.g. interim, progress, summary, annual or final. Give the inclusive dates when a specific reporting period is covered.)

Contract Report

8. SPONSORING ACTIVITY (The name of the department project office or laboratory sponsoring the research and development – include address.)

Defence Research and Development Canada – Suffield
P.O. Box 4000, Station Main
Medicine Hat, Alberta T1A 8K6

9a. PROJECT OR GRANT NO. (If appropriate, the applicable research and development project or grant number under which the document was written. Please specify whether project or grant.)	9b. CONTRACT NO. (If appropriate, the applicable number under which the document was written.)
	W7702-115043/A

10a. ORIGINATOR'S DOCUMENT NUMBER (The official document number by which the document is identified by the originating activity. This number must be unique to this document.)	10b. OTHER DOCUMENT NO(s). (Any other numbers which may be assigned this document either by the originator or by the sponsor.)
ASLAM-RP-53-4754	DRDC Suffield CR 2013-070

11. DOCUMENT AVAILABILITY (Any limitations on further dissemination of the document, other than those imposed by security classification.)

Unlimited

12. DOCUMENT ANNOUNCEMENT (Any limitation to the bibliographic announcement of this document. This will normally correspond to the Document Availability (11). However, where further distribution (beyond the audience specified in (11) is possible, a wider announcement audience may be selected.))

Unlimited

13. ABSTRACT (A brief and factual summary of the document. It may also appear elsewhere in the body of the document itself. It is highly desirable that the abstract of classified documents be unclassified. Each paragraph of the abstract shall begin with an indication of the security classification of the information in the paragraph (unless the document itself is unclassified) represented as (S), (C), (R), or (U). It is not necessary to include here abstracts in both official languages unless the text is bilingual.)

The objective of the Appearance-based Simultaneous Localization And Mapping (ASLAM) project is the research and development of an Appearance-Based Simultaneous Localization and Mapping system for day/night operations in indoor and outdoor environments. These algorithms would perform place recognition based on sensor data gathered from an Unmanned Ground Vehicle (UGV) as it travels through the environment. When the vehicle returns to a previously visited scene, the ASLAM algorithm would recognize the scene, update its internal representation, report this to the UGV, and finally provide information to aid in closing the loop with geometric Simultaneous Localization And Mapping (SLAM).

The key objectives of Task 4.4 are to characterize the performance of the ASLAM system under different settings and to determine the optimal system parameters, with detailed Receiver Operator Characteristic (ROC) analysis.

This report describes the findings of the ROC analysis. The ROC curves illustrate graphically how the probability of detection and the false alarm rate vary at different thresholds, and how the key system parameters affect the performance.

L'objectif du présent contrat est la recherche et le développement d'un système de localisation et de cartographie en temps réel basé sur l'apparence pour les opérations menées de jour et de nuit, à l'intérieur comme à l'extérieur. Ces algorithmes doivent effectuer une reconnaissance de l'endroit basée sur les données recueillies par le capteur de l'UGV alors que celui-ci se déplace dans un environnement donné. Lorsque le véhicule revient sur une scène déjà visitée, l'algorithme ASLAM reconnaît la scène, met à jour sa représentation interne, la communique au UGV et, enfin, dispose d'un mécanisme pour fermer la boucle à l'aide du SLAM géométrique.

Les principaux objectifs de la tâche 4.4 sont de caractériser le rendement du système ASLAM sous divers réglages et de déterminer les paramètres optimaux du système à l'aide d'une analyse détaillée de la fonction d'efficacité du récepteur (FER).

Le présent rapport comprend les résultats de l'analyse FER. Les courbes de la FER illustrent comment la probabilité de détection et le taux de fausses alarmes varient en fonction de certains seuils et quelle incidence les principaux paramètres du système ont sur le rendement.

14. KEYWORDS, DESCRIPTORS or IDENTIFIERS (Technically meaningful terms or short phrases that characterize a document and could be helpful in cataloguing the document. They should be selected so that no security classification is required. Identifiers, such as equipment model designation, trade name, military project code name, geographic location may also be included. If possible keywords should be selected from a published thesaurus, e.g. Thesaurus of Engineering and Scientific Terms (TEST) and that thesaurus identified. If it is not possible to select indexing terms which are Unclassified, the classification of each should be indicated as with the title.)

Appearance-based Simultaneous Localization And Mapping ; ASLAM; UGV; imultaneous Localization And Mapping; SLAM